Detrital carbonate minerals in Earth's element cycles

Gerrit Müller*[,a], Janine Börker[b], Appy Sluijs [a], Jack J. Middelburg [a]

[a] *Department of Earth Sciences, Utrecht University, The Netherlands*

[b] *Institute for Geology, CEN (Center for Earth System Research and Sustainability), Universität Hamburg, Germany*

g.muller@uu.nl

janine.boerker@uni-hamburg.de

A.Sluijs@uu.nl

J.B.M.Middelburg@uu.nl

* *corresponding author: Gerrit Müller*

Mail: g.muller@uu.nl

Address: Vening Meineszgebouw A, Princetonlaan 8a, 3584 CB Utrecht, The Netherlands

Abbreviations: IC: Inorganic carbon, PIC: Particulate inorganic carbon, DIC: Dissolved inorganic carbon, POC: Particulate Organic Carbon, DOC: Dissolved Organic Carbon, SOC: Soil organic carbon, TC: Total river carbon, SVM: Support Vector Machine, MGGP: Multi-Gene Genetic Programming, SR: Symbolic Regression, RMSE: Root mean squared error, MC: Monte Carlo, VI: Variable Influence, fwm: flux-weighted mean, med: median, mod: modelled, wo: without, S: related to change in sediment discharge, D: related to damming, SC: Source Carbonate, hdi: human development index, gdp: gross domestic product, nli: night light index, pop: population count, N: Number of simulations.

Key points:

- The present day riverine detrital carbonate flux from land to sea is 3.1 ± 0.3 Tmol C/y (= 0.037 Pg C/y).
- Associated calcium, alkalinity and strontium contribute significantly to their global biogeochemical cycles.
- Damming reduced the riverine PIC flux by 25 % (from naturally 4.1 ± 0.5 Tmol C/y = 0.049 Pg C/y).

Abstract. We investigate if the commonly neglected riverine detrital carbonate fluxes might balance several chemical mass balances of the global ocean. Particulate inorganic carbon (PIC) concentrations in riverine suspended sediments, i.e., carbon contained by these detrital carbonate minerals, was quantified at the basin and global scale. Our approach is based on globally representative datasets of riverine suspended sediment composition, catchment properties and a two-step regression procedure. The present day global riverine PIC flux is estimated at 3.1 ± 0.3 Tmol C/y (13% of total inorganic carbon export and 4 % of total carbon export), with a flux-weighted mean concentration of 0.26 ± 0.03 wt%. The flux prior to damming was 4.1 ± 0.5 Tmol C/y. PIC fluxes are concentrated in limestone-rich, rather dry and mountainous catchments of large rivers in Arabia, South East Asia and Europe with 2.2 Tmol C/y (67.6 %) discharged between 15 °N and 45 °N. Greenlandic and Antarctic meltwater discharge and ice-rafting additionally contribute 0.8 ± 0.3 Tmol C/y. This amount of detrital carbonate minerals annually discharged into the ocean implies a significant contribution of calcium (~ 4.75 Tmol Ca/y) and alkalinity fluxes (~ 10 Tmol(eq)/y) to marine mass balances and moderate inputs of strontium (~ 5 Gmol Sr/y), based on undisturbed riverine and cryospheric inputs and a dolomite/calcite ratio of 0.1.

Magnesium fluxes (~ 0.25 Tmol Mg/y), mostly hosted by less-soluble dolomite, are rather negligible. These unaccounted fluxes help elucidating respective marine mass balances and potentially alter conclusions based on these budgets.

Plain Language Summary. Earth surface conditions, including climate and sea level, are largely controlled by the cycling of carbon and biogeochemically coupled elements. However, most elemental budgets cannot be consentaneously balanced for the present state. Here, we investigate the possible role of riverine carbonate minerals in biogeochemical cycles. We derive individual river basin export fluxes, the global export flux to the ocean and its reduction by human influence, utilizing state-of-the-art regression techniques and published global-scale datasets. Results point to a significance of riverine detrital carbonates for the global mass balances of carbon, calcium, alkalinity and strontium, which might help solving this long-standing problem.

Graphical Abstract

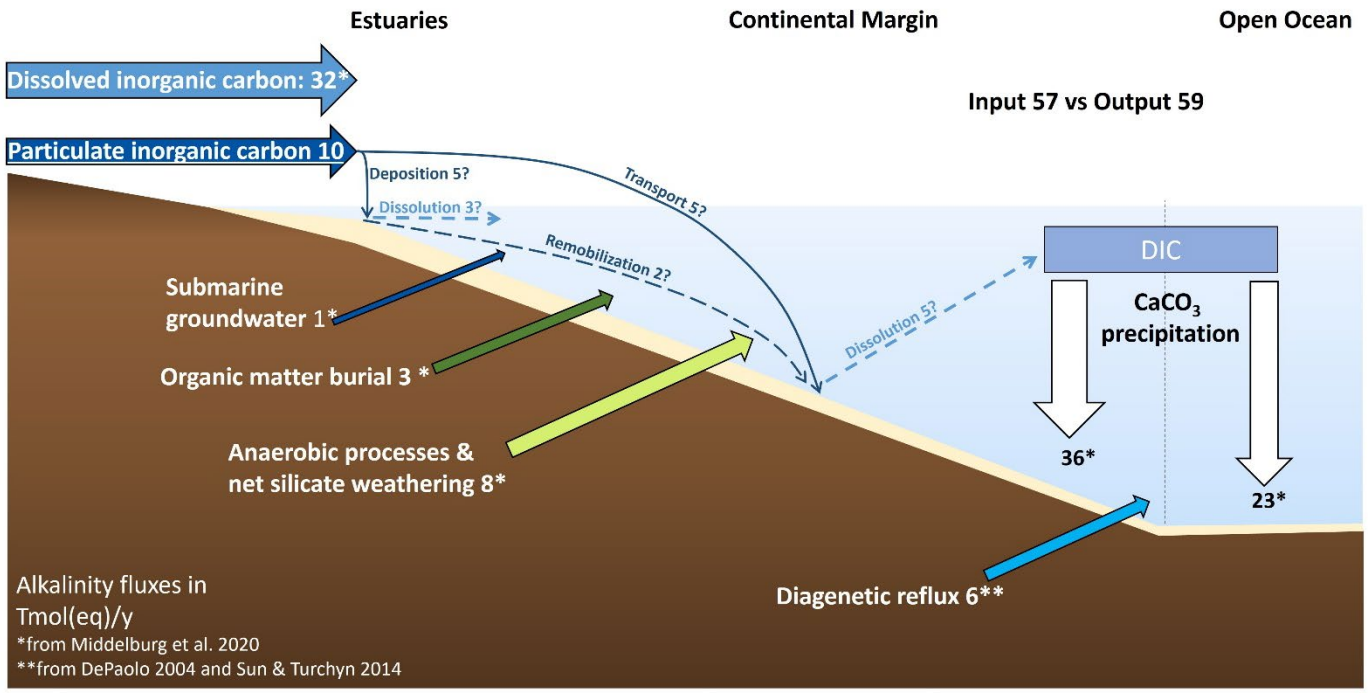

1 Introduction

Erosion and weathering of Earth's surface not only shape landscapes, but also influence the global carbon cycle, thereby maintaining the habitability of our planet (Berner et al., 1983; Ebelmen, 1845; Ferrier and West, 2017; Penman et al., 2020; Urey, 1952; West et al., 2005). Oceanic mass balances of carbon (C) and biogeochemically coupled elements provide a powerful tool to investigate these processes and their role in the Earth system globally and over longer time-scales (classically > 100 ka) (Berner and Berner, 2012; Dickens, 2001; Krabbenhöft et al., 2010; Tipper et al., 2010). They also allow quantification of hardly measurable processes, such as global rates of marine carbonate burial or hydrothermal activity (Shalev et al., 2019; Tipper et al., 2006; van der Ploeg et al., 2019). However, some of the most prominent and most frequently considered budgets presented in that context remain unbalanced and/or highly debated, such as those of Ca, Mg, Sr and alkalinity (Berner and Berner, 2012, 1987; Gislason et al., 2006; Jones et al., 2012; Krabbenhöft et al., 2010; Lebrato et al., 2020; Milliman, 1993; Tipper et al., 2010, 2006). This is usually explained by disequilibrium, i.e., the present state strongly differs from average Pleistocene conditions, by proposing a variety of smaller-scale marine processes and/or by invoking yet unaccounted input fluxes (Krabbenhöft et al., 2010; Middelburg et al., 2020; Milliman, 1993; Shalev et al., 2019; Tipper et al., 2010).

For most marine mass balances, riverine dissolved loads are traditionally considered the only major input term, reflecting the catchment-integrated result of chemical rock weathering as transported by the Earth-spanning fluvial networks (Berner and Berner, 2012, 1987). Some authors recognized submarine groundwater discharge as another important flux to the ocean with a probable magnitude of 0.7 to 6 % of the global river discharge (Mayfield et al., 2021; Milliman, 1993; Zhou et al., 2019). In addition to these dissolved inputs, it is generally accepted that organic and biogenic riverine particles exert major control on the biogeochemical cycling of carbon (C), nitrogen (N) and phosphorous (P) (Berner, 1999, 1982;

Boyer and Howarth, 2008; Froelich et al., 1982; Hilton and West, 2020), and of silicon (Si) (Conley, 2002; Sutton et al., 2018). Moreover, the importance of ions and complexes sorbed to the surfaces of riverine sediments was highlighted (Berner et al., 1983; Tipper et al., 2021). A similar importance was proposed for particulate inorganic forms (mineral detritus) of silicon (Si) (Mackenzie and Garrels, 1966, 1965), calcium (Ca) (Gislason et al., 2006), strontium (Sr) (Hong et al., 2020; Jones et al., 2012), iron (Fe) (Luo et al., 2020; Poulton and Raiswell, 2002) and other elements (e.g., Abbott et al., 2019; Jeandel et al., 2011), based on experimental and field-measured element release rates. Recently, based on a limited dataset, Middelburg et al. (2020) suggested that riverine particulate inorganic carbon (PIC) fluxes to the ocean may be about 1/3 of riverine dissolved inorganic carbon (DIC) fluxes and that the ocean alkalinity budget is close to balance when this is considered an additional alkalinity input. While basaltic minerals, ashes and glasses of volcanic origin are currently considered to be the major host minerals of particulate Ca and Sr fluxes (Gislason et al., 2006; Jones et al., 2012; Torres et al., 2020), significant riverine PIC fluxes would imply substantial additional Ca, Sr and Mg delivery in particulate forms.

Carbonate dissolution and recrystallization are well known to occur in estuaries (Aller, 1982; Gattuso et al., 1998; Santos et al., 2019) and the ocean (Krumins et al., 2013; Milliman, 1974; Sulpis et al., 2017), providing evidence for the (partial) release of Ca, Mg, Sr, inorganic C (IC) and alkalinity from detrital sources to the oceanic inventories. Dissolution of PIC in the ocean could, thus, represent a major missing term in oceanic mass balances, potentially altering the conclusions deduced from those budgets (e.g., Berner and Berner, 2012; Krabbenhöft et al., 2010; Paytan et al., 2021; Tipper et al., 2006, 2010). Notably, recrystallization within the sediment column, i.e., dissolution and direct re-precipitation, may result in an exchange of elements and isotopes between PIC and seawater (DePaolo, 2004; Fantle et al., 2010; Paytan et al., 2021).

High solubility and rapid dissolution kinetics of carbonate minerals cause the dominant mass of IC to be transported in dissolved form (Lasaga, 1984). Therefore, the significance of detrital carbonate minerals in river sediments is often neglected. However, detrital carbonates are commonly observed constituents of suspended sediments in rivers (Mackenzie and Garrels, 1966; Müller et al., 2021a) and even authigenic carbonate production in calcite-saturated rivers is common (Grosbois et al., 2001; Kempe and Emeis, 1985; Négrel and Grosbois, 1999). Such authigenic carbonate formation on land represents a (temporary) sink of weathering-derived cations, alkalinity and carbon, with implications for the location of gas exchange and global mass balancing (Rovan et al., 2021; Zhao et al., 2016). Sr-isotopic constraints suggest that 30 – 50 % of the carbonate minerals within the Gulf of Lyon sediments are detrital, even more during glacial periods (Pasquier et al., 2019). Additionally, the isotopic composition of carbonates from turbidites in the Bengal fan, one of the largest sediment dispersal systems on earth (Mouyen et al., 2018), suggests a mixture of biogenic (> 85 wt%), detrital (up to 10 wt%) and diagenetic (1.2 – 4 wt%) origin (France-Lanord et al., 2018). This indicates that the PIC delivery may indeed be a relevant flux to the marine realm, but its size and dissolving fraction remain unclear because a global assessment is lacking.

We aim to better constrain these important numbers based on several approaches. First, we establish a first-order calculation based on published average PIC and CaO concentrations and sediment fluxes. Next, we quantify PIC concentrations and fluxes globally at the basin-scale, using published datasets of riverine suspended sediment and catchment characteristics, and a two-step regression procedure, involving regressive classification and symbolic regression (for details see section 2.2; Regression and Upscaling & Supplementary Information SI 2). Controlling factors of the global PIC flux, human influence and the fate of the delivered detrital carbonates in the ocean are then discussed, including implications for oceanic mass balances and carbon cycling.

2 Methods and procedures

To calculate the global PIC flux, we need a gapless set of PIC concentrations and sediment fluxes of all rivers in the world, which is not realistically achievable from measurements. However, the latter can be generated using advanced models that provide suspended sediment fluxes of global rivers in space and time, based on water balance and catchment properties (WBMSed 2.0, Cohen et al., 2014). The WBMSed 2.0 provides anthropogenically disturbed suspended sediment flux data, as well as natural background values. These data, along with the locations of the river mouths, were taken from a compilation of the *GlobalDelta* project (Nienhuis et al., 2020). No such model is available for PIC concentrations yet. Hence, we here develop a statistical, spatially-explicit model that predicts PIC concentrations from catchment properties. Modelled PIC concentrations were combined with both, the natural and the anthropogenically disturbed suspended sediment fluxes (WBMSed 2.0) to arrive at the corresponding PIC fluxes.

Annual median PIC concentrations were calculated for all locations in the GloRiSe v1.1 database (Müller et al., 2021b) from direct measurements, mineralogical and petrographic observations or empirically from major element composition (Supplementary Information SI 1). The uncertainty of these concentrations was defined as the mean relative deviation of single measurements from the flux-weighted mean of available time-series (Müller et al., 2021b). A large set of hydro-environmental and physiographic variables was derived from the HydroBasins database (Linke et al., 2019) by spatially assigning each GloRiSe-location to the corresponding sub-basin (at Pfafstetter level 7). Annual averages for the upstream catchment of nine variables were selected based on correlation analysis and/or a causal link to PIC concentrations (Supplementary Information SI 1). These variables cover topography, vegetation, hydrology, climate and human impact (Table 1). As the carbonate in the catchment is the source of riverine PIC, a proper indication of this ‘source carbonate’ (SC) was extracted

159 from global maps of lithology (GLiM, Hartmann and Moosdorf, 2012), unconsolidated
160 sediments (GUM, Börker et al., 2018) and soils (WISE, Batjes, 2012). For soils, the carbonate
161 content was given directly, while for each rock and sediment class a global representative
162 estimate of the carbonate content was taken from literature (Supplementary Information SI 1).
163 Area-weighted upstream averages were calculated individually for the carbonate content of
164 GliM, GUM and WISE in each basin. Next, these were summed and normalized to 100 % to
165 represent the SC, i.e., carbonate available to be transported as PIC. All the predictor variables
166 are summarized in Table 1. Catchments with SC < 10 % were assumed to be PIC-free, as
167 dissolution usually dominates over detrital carbonate transport in (undersaturated) rivers (see
168 1 Introduction).

Table 1 *Predictor variable selection to model PIC concentrations. Variables are taken from HydroBasins (Linke et al., 2019), except for the potential source carbonate, which was calculated from global soil, sediment and lithological maps* (Batjes, 2012; Börker et al., 2018; Hartmann and Moosdorf, 2012)*. All variables represent the upstream-average of a specific HydroBasins sub-basin at Pfafstetter level 7. Abbreviations: hdi: human development index, gdp: gross domestic product, nli: night light index, pop: population count.*

Topography & Vegetation	Underground & Humans	Climate & Hydrology
Elevation	Potential source carbonate (rock, sediment, soil)	Precipitation
Upstream catchment area	Soil organic carbon content	Temperature
Forestation	Human factor (log(hdi+gdp+nli+pop))	Extent of water bodies (rivers, lakes, reservoirs)
Bare areas (rock, desert, tundra, open shrub land)		

169

170 **2.1 Regression & Upscaling**
171

172 To estimate PIC concentrations in the remaining ~65 % of the global suspended sediment
173 discharge, we employed a two-step regression procedure consisting of (I) a qualitative
174 indication of the presence of PIC in a catchment (yes/no) and (II) a quantitative regressive

175 estimation of the PIC concentration. This two-step procedure was necessary because PIC
176 concentrations are not only log-normally distributed, but also frequently close or equal to zero,
177 thus hampering the regression procedure, which is a well-known problem in ecology (Fletcher
178 et al., 2005).

179 For the qualitative model, we applied a Support Vector Machine (SVM), a standard
180 technique from the MATLAB 2019b Machine Learning toolbox. This model was trained and
181 forced by only five variables, because SVMs have been found to achieve better results with
182 less variables (Kitsikoudis et al., 2013). We chose to use SC, precipitation, elevation,
183 forestation and human factor, covering the most diverse aspects of sources and preservation
184 potential of PIC. PIC concentration was assumed not present if it was below 0.1 wt%,
185 approximating the uncertainty of most measurements included in *GloRiSe*. SVM was chosen,
186 because it performed slightly better than alternative methods, such as logistic regression and
187 ensemble techniques.

188 For the quantitative model, symbolic regression (SR) by means of multi-gene genetic
189 programming (MGGP) was used, providing a fully data-driven tool to find both the model
190 structure and its parameters. SR was chosen, because it performed better than simple linear
191 regression or alternative machine learning techniques (available e.g., in the MATLAB
192 Regression Learner Toolbox) in terms of both, accuracy and precision. The implemented SR-
193 algorithm pseudo-randomly creates linear combinations of (potentially non-linear) terms,
194 which are tested and evolved to best fit the observed PIC concentrations as assessed by the root
195 mean squared error (*GPTIPS* 2.0, Searson et al., 2010). Thus, SR is able to cover non-linear
196 relationships between the variables and its performance seems comparable to artificial neural
197 networks, while it still results in comparably simple equations that can be related to the
198 governing processes (Gandomi et al., 2015; Jin et al., 2019; Kitsikoudis et al., 2013). Variable
199 selection and SR intrinsically determine the importance of individual variables for, and their

200 direction of relationship to PIC concentrations, which we quantitatively assess using the linear
201 correlation coefficient and coefficient of determination (R and R^2, respectively, at $p < 0.01$)
202 between the median result of 830 accepted Monte Carlo simulations and each variable. This
203 method reduces biases due to multi-collinearity and non-linearity and is commonly applied to
204 the evaluation of canonical correlations analyses (Kuylen and Verhallen, 1981).

205 The global riverine PIC flux is the sum of the products of sediment fluxes and PIC
206 concentrations in each basin draining directly to the coastal ocean. For a proper re-estimation
207 and uncertainty analysis, the regression and prediction procedure was repeated 2,000 times
208 with a (pseudo-)random perturbation of sediment fluxes and PIC concentrations within the
209 range of their respective uncertainties, including the full model derivation via SVM and SR.
210 The final result is the mean of 830 accepted simulations that produced less than 0.3 % outliers
211 in respect to the 10 % and 90 % percentile (10 of 3364 coastal basins) and its uncertainty is the
212 standard deviation of these models (Koehler et al., 2009). For comparison, we also provide
213 literature-based first-order estimates of riverine PIC fluxes (Supplementary Information S3).
214 Because much less detailed data is available for atmospheric and cryospheric PIC
215 contributions, these fluxes were estimated using published PIC concentrations and sediment
216 fluxes (Supplementary Information S3).

3 Results

We calculate that currently 3.1 ± 0.3 Tmol PIC are annually discharged to the coastal ocean. The pre-human flux was 4.1 ± 0.5 Tmol PIC/y (Fig. 1), accounting for damming and soil erosion (by the underlying WBMSed 2.0 model (Cohen et al., 2014, 2013)). The 25 % reduction is dominated by particle retention in reservoirs. The uncertainty of 10 % appears low, considering the much larger uncertainty of sediment fluxes (50 %), observed PIC concentrations (50 %) and

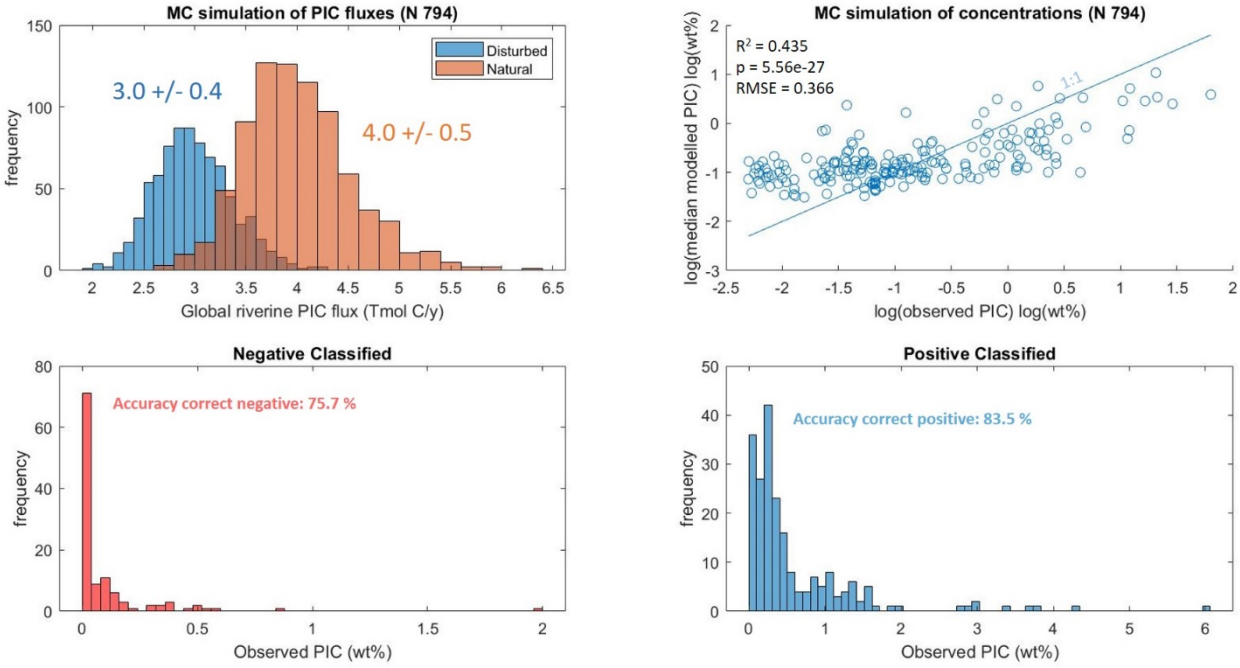

Figure 1*: Results (upper) and performance (lower) of the Monte Carlo (MC)-refined regression procedure. Histograms (upper left panel) show the distribution of natural and anthropogenically disturbed global PIC fluxes in Tmol C/y (times 0.012011 yields Pg/y). The upper right panel assesses the performance of the quantitative prediction via SR (1:1 line = perfect prediction). The lower panels evidence the performance of an exemplary qualitative model (left: negative classifications (= No PIC present, correct predictions are < 0.1 wt%); right: positive classifications (= PIC present, correct predictions are > 0.1 wt%). N is the number of accepted MC simulations. RMSE is the root mean squared error.*

Table 2 *Comparison of the herein presented results and literature-based estimates of global average PIC concentration (cPIC, flux-weighted mean, median and mixture of median and mean, respectively), suspended sediment discharge (fTSS, global sum) and PIC flux (fPIC, global sum). References: 1: Meybeck (1982), 2: Viers et al. (2009), 3: Savenko (2007), 4: Bayon et al. (2015), 5: Beusen et al., (2005), 6: Milliman and Farnsworth (2011), 7: Syvitski and Kettner (2011), 8: Cohen et al. (2014), 9: Middelburg et al. (2020) based on Canfield, (1997) and Beusen et al. (2005), 10: Meybeck (1993), 11: Journet et al. (2014), 12: Jickells et*

al (2005), 13: Overeem et al. (2017), 14: Raiswell et al. (2008), 15: Wadham et al. (2013). Abbreviations: med: median, fwm: flux-weighted mean, obs: observations, wo: without,. 'Literature' indicates values and ranges that were calculated from published values ('first-order' estimates, Supplementary Information SI 2, grey columns). 'This study' refers to values we derived in this contribution (2 Methods & Procedures, Supplementary Information SI 1). Bold numbers indicate the values suggested for further use. Conversion to Pg/y by a factor 0.012011.

Variable (unit)	**cPIC (wt%)**	**cPIC (wt%)**	**cPIC (wt%)**	**fTSS river (Gt/y)**	**fPIC river, pre-human (Tmol C/y)**	**fPIC river, present day (Tmol C/y)**	**fPIC river, actual (Tmol C/y)**	**fPIC atmosphere (Tmol C/y)**	**fPIC cryosphere (Tmol C/y)**
Value	**0.26**	0.42	0.7	16	**4.1**	**3.1**	10.4	**0.25**	**0.78**
Range	**0.24 – 0.28**	0.1 – 0.7	0.4 - 1	12 - 20	**3.6 – 4.6**	**2.8 – 3.4**	4.0 – 16.7	**0.10 – 0.40**	**0.48 – 1.12**
Reference	This study (fwm, model)	This study (med, obs.)	Literature (1 – 4)	Literature (5-8)	This study (model)	This study (model)	Literature (1 – 10)	Literature (11,12)	Literature (13-15)

quantitatively modelled PIC concentrations (factor 4) (Supplementary Information S2.3). The reason is the low uncertainty of PIC presence: correct negative classifications (= no PIC present) (75.7 % accuracy) have a lower range of 0 – 0.1 wt% and basins with less than 10 % source carbonate are assumed to have a PIC concentration and error of 0 wt%, reducing variability of results and errors. Positive classifications (= PIC present) are similarly accurate (83.5 %). Moreover, modelled PIC concentrations are within a smaller range than observed values, i.e., the model is biased. Very small values, i.e., PIC < 0.1 wt%, will not drastically affect results, especially because the global flux is dominated by a few large rivers (see below). Miscalculations in PIC-rich rivers, could be more critical to the assessment, e.g., the Rhone river is a comparably small river in terms of sediment discharge, but a major contributor to the

234 global PIC flux because of high PIC concentrations. However, for most of the important rivers
235 measurements are available, and thus this uncertainty is accounted for (Supplementary
236 Information S2.3). Therefore, the global flux and flux-weighted average concentrations are
237 rather robust. Notably, these uncertainties do not account for inaccuracies in the input datasets.

238 For instance, the global lithological map (*GLiM*) has an accuracy of only ~ 60%
239 compared to point observations (Hartmann and Moosdorf, 2012). The flux-weighted mean PIC
240 concentration of 0.26 ± 0.03 wt% is lower than the median of PIC-bearing rivers only (0.41 ±
241 0.01 wt%, excluding PIC-free rivers) implying ~40 % of the riverine sediment flux to be PIC-
242 free. Both are statistically indistinguishable from the median of observed basinal averages (0.35
243 ± 0.3 wt%), covering ~ 35 % of the global sediment flux (Cohen et al., 2014). Additionally,
244 some authors used mean values, which are more susceptible to outliers caused by small rivers
245 and are typically higher than medians (because of log-normal distributions). High PIC
246 concentrations are rarely found in rivers with high discharge, except for a few large rivers
247 draining markedly dry (e.g., the Nile and Euphrates-Tigris systems) and/or mountainous (e.g.,
248 the Indus system) catchments (Fig. 2).

249 From a total of 3365 catchments considered, the biggest 862 basins contribute ~ 99 %
250 of the total riverine PIC flux, while the biggest 10 catchments, situated in South-East Asia,
251 Arabia, Europe and North America already sum up to ~ 53 %. The Euphrates-Tigris system
252 (13.3 %), the Indus (10.3 %) and the Nile (8.9 %) alone contribute 32.6 % of the total global
253 PIC flux, followed by Yangtze (4.5 %), Salween (4.4%), Colorado (USA, 3.4 %), Rhone
254 (2.8 %), Huanghe (2.1 %), Mississippi (2.0 %) and the Ganga-Brahmaputra system (1.6 %).

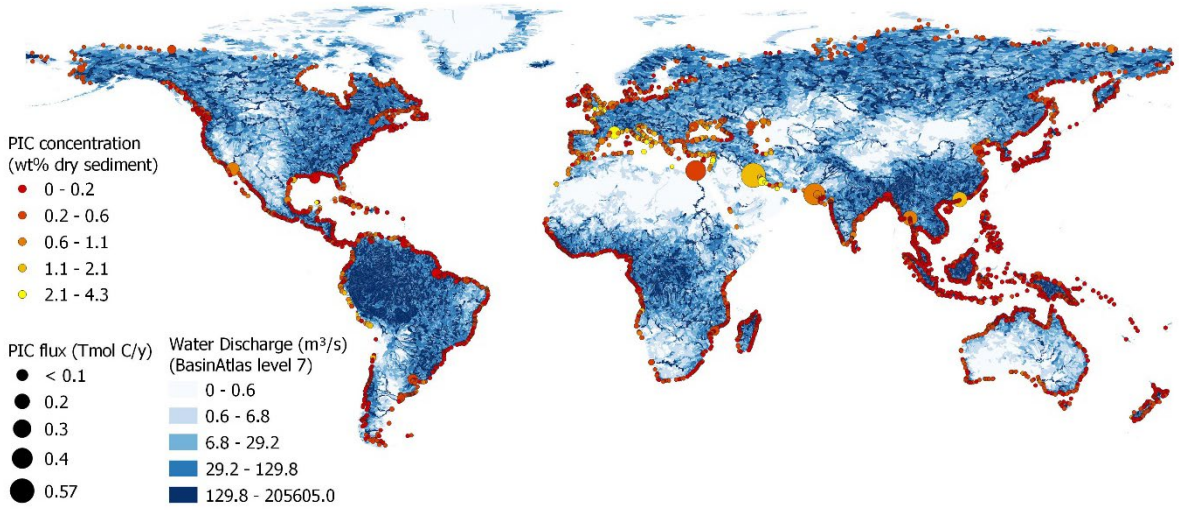

Figure 2 *Map of the model results. Point data along the coast are the result of this study (Mean of 794 accepted Monte Carlo simulations). Size scales with the magnitude of the PIC flux (Tmol C/y), based on pre-human sediment discharge) and color is related to PIC concentration (wt %). For comparison, blue colors indicate natural annual mean water discharge (m^3/s) (Linke et al., 2019). Conversion of fluxes to Pg/y by a factor 0.012011.*

About two-thirds (2.7 Tmol PIC/y) is delivered to the coastal ocean between 15 °N and 45 °N, contrasting riverine DIC, OC, total solute and bulk sediment fluxes (Hartmann et al., 2014; Ludwig et al., 1996; Milliman and Farnsworth, 2011). The anthropogenic reduction of the global PIC flux is dominated by the decreasing contribution of the Nile due to intense damming (~ 8 of 25 %).

The present PIC flux related to atmospheric dust deposition is 0.25 ± 0.15 Tmol C/y, which is ~ 8 % of the riverine PIC flux and ~ 0.3 % of the total riverine carbon flux (~ 71 Tmol C/y, Supplementary Information S3). Thus, the atmospheric contribution is negligible in global mass balances. PIC related to meltwater discharge and ice-rafted debris from Greenland and Antarctica together contribute another 0.8 ± 0.3 Tmol PIC/y, which is ~ 26 % of the present day riverine PIC flux and ~ 1 % of the total river carbon flux (Supplementary Information S3). In total, ~ 4 Tmol PIC arrive in the ocean annually (~ 5 Tmol when considering natural river discharge, see Table 1).

4 Discussion

4.1 Natural controls of PIC and their variation through time

The relevance of each variable to the model was assessed through the coefficients of correlation and of determination between the individual variable and the median model outcome, being independent of non-linearity and multi-collinearity (Fig. 3). A strong positive influence of SC on PIC concentrations is eminent from these procedures (+ 38 %, Fig. 3). SC includes carbonate from soils (~ 3 % carbonate on average) and unconsolidated sediments (~ 2 – 4 %) but is dominated by lithological (bedrock) contributions (~ 20 % on average). This is because terrestrial carbonate weathering is dissolution-dominated, which arises from fast dissolution and high solubility (Lasaga, 1984; Morse and Arvidson, 2002). This contrasts with the precipitation-dominated behavior of silicates, producing clay minerals and oxides characteristic to soil assemblages (Brantley et al., 2008; Lasaga, 1984; Ma et al., 2011; Morse and Arvidson, 2002).

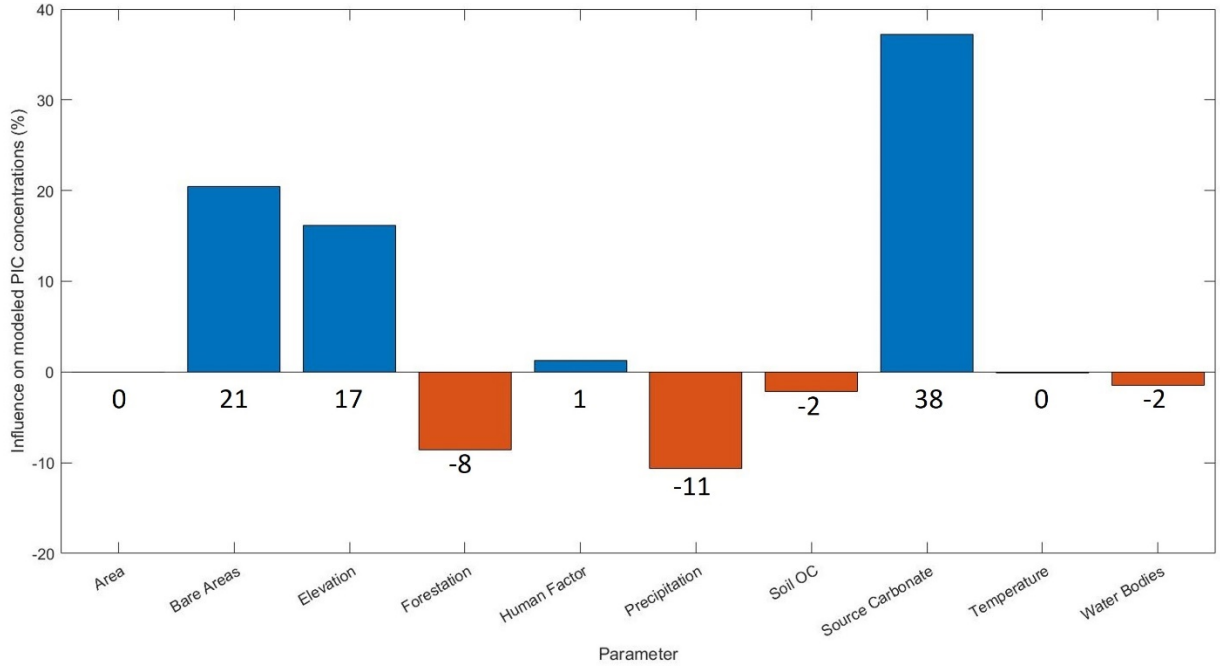

Figure 3 *Relative importance of the different variables to our model results as assessed by the coefficient of determination (R^2) between the variable in question and the median result of 794*

high-quality Monte Carlo simulations. The correlation coefficient gives the direction of influence (orange: negative, blue: positive). Individual values are indicated above the bars. OC: Organic Carbon. Variables as in Table 1.

Generally, riverine suspended sediment is a mixture of source rocks, their solid weathering products (soil and sediment), organic matter and material of anthropogenic origin, with additional in-stream processing. Thus, the differences between SC and PIC may arise from preferential dissolution of carbonates compared to silicates in the weathering zone (= soil) before erosion, and also from in-stream dissolution (Dornblaser and Striegl, 2009), precipitation (e.g., Kempe and Emeis, 1985; Négrel and Grosbois, 1999) and particle sorting during transport (e.g., Bouchez et al., 2011; Garzanti et al., 2011). According to our results, humans did not (yet) influence PIC concentration significantly on a global scale (influence of human factor is only 1%, Fig. 3), while they severely reduced PIC fluxes through their impact on suspended sediment discharge (see section 4.2 Human activities and riverine carbon). A thick soil cover can only develop if chemical weathering rates exceed material removal by erosion (Ferrier and West, 2017; West, 2012), and it is promoted by biological activity. Especially forestation stabilizes the soil, disintegrates pristine rocks and introduces organic acids and ligands, increasing mineral solubilities (Brantley et al., 2017; Calmels et al., 2014).

This view is supported by the negative impact of variables in favor of soil formation and dissolution, such as precipitation (- 11 %) and forestation (- 8 %). In contrast, the organic carbon content of soils and temperature, which may influence dissolution kinetics, do not seem to play a major role for PIC concentrations, nor do catchment size or the extent of water bodies, (relatable to the residence time of the particles within the fluvial system). The more prominent influence of (rock) erosion on PIC concentrations is evident from the large influence of related variables, namely, elevation (+ 17 %) and the extent of bare areas (+ 21 %). Rapidly eroding, mountainous terrains are characterized by fast, efficient transport and diminutive sediment

storage (Hilton and West, 2020; Milliman and Syvitski, 1992), limiting both the extent of soil formation (Dixon and von Blanckenburg, 2012; Jenny, 1941) and in-stream dissolution.

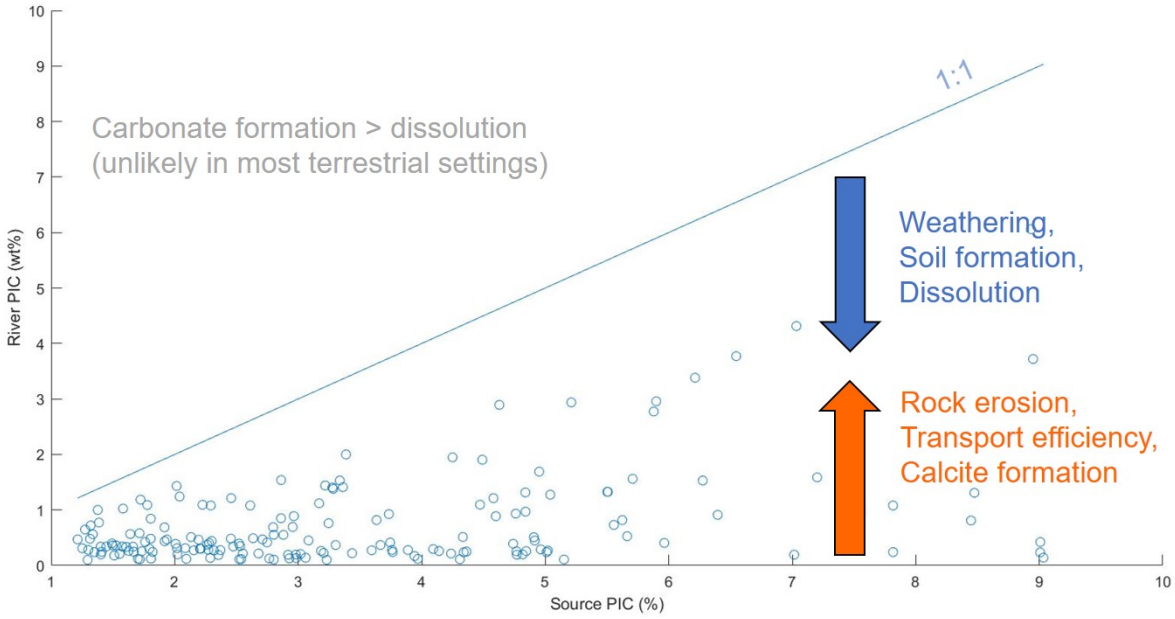

Figure 4 *Relationship of river PIC and source PIC. Source PIC (12 % of SC) includes sediment and soil contributions but is dominated by rocks. In-stream dissolution and contributions of weathered material decrease river PIC, while rock erosion has a pronounced positive effect by contributing source rock. Transport efficiency and in-stream precipitation can further enhance PIC concentrations at the river mouth. The unit of Source PIC (%) is wt% PIC in the given percentage of carbonate within the upstream outcrop area.*

This interpretation that PIC concentrations increase with erosion is apparently inconsistent with increasing carbonate dissolution following pyrite oxidation and sulfuric acid production upon accelerated erosion as observed in shale-dominated terrains (Bufe et al., 2021; Calmels et al., 2007; Torres et al., 2014). However, we do not only consider shale-rich, but all carbonate-bearing (> 10 %) terrains in this analysis, which could obscure such relationships. Such an apparent inconsistency was noted for other global scale compilations as well (Bufe et al., 2021). Moreover, PIC is predominantly produced by the physical disintegration of pristine rocks and soils, while this same process promotes dissolution and oxidation kinetics. Thus, trends in PIC concentrations and carbonate dissolution do not strictly oppose each other but may even covary in rapidly eroding terrains.

In summary, the rather slowly changing (10^3 – 10^5 y) tectonic, physiographic and

lithological settings seem to exert a dominant control on PIC concentrations as demonstrated by the eminent role of SC and elevation in our model. Superimposed on this base-line situation, much faster variations in climatic and vegetation patterns seem to affect the relative contributions of weathered, PIC-poor soil and pristine, PIC-rich source rock.

Although heavily discussed (Caves Rugenstein et al., 2019; Foster and Vance, 2006; Willenbring and Von Blanckenburg, 2010), many observations suggest that soil formation and/or chemical weathering decreased during cold, dry periods (Berner et al., 1983; Dixon et al., 2016; Jenny, 1941; Schachtman et al., 2019), potentially increasing the ratio of pristine source rock to weathered soil in suspended sediments, thus, the riverine PIC flux. Moreover, glacial activity during cooler periods may accelerate erosion, thus, PIC production and potentially preservation (because of decreased residence times). This is supported by an increase of the detrital carbonate fraction in glacial sediments of the Gulf of Lyon, compared to sediments deposited during interglacial periods (Pasquier et al., 2019). An indication of increased cryogenic PIC deposition in response to ice-sheet dynamics is provided by the so-called 'Heinrich-events', which are unusual accumulations of coarse carbonate-rich detritus in marine sediment (Bond and Lotti, 1995; White et al., 2016). In contrast, thawing permafrost exposes old, but fresh organic matter that is rapidly respired (e.g., Walz et al., 2017), potentially increasing PIC dissolution (Aller, 1982; Archer et al., 1989; Calmels et al., 2014; Oelkers et al., 2011; Zolkos et al., 2018). Consistently, although not solely related to carbonate weathering, an increased riverine export of dissolved inorganic carbon in response to the recent warming was reported from large Arctic rivers (Drake et al., 2018; Zolkos et al., 2020).

However, recent observations and theories challenge this simple view (Caves Rugenstein et al., 2019; Foster and Vance, 2006; Willenbring and Von Blanckenburg, 2010), implying more complex and transitional spatio-temporal dynamics of erosion (Chen et al., 2018; Foreman et al., 2012; van de Schootbrugge et al., 2020) and carbonate weathering

(Gaillardet et al., 2019; Zeng et al., 2019) and, consequently, of riverine inorganic carbon export. Additionally, environmental conditions and, consequently, carbonate dissolution in the (coastal) ocean are expected to change over multiple time-scales, ranging from seasons and decades (Cai et al., 2011; Wallace et al., 2014) to geological time-scales (Broecker, 1982; Ganeshram et al., 2000; Sluijs et al., 2013), with implications for the magnitude and timing of contribution of PIC to oceanic inventories.

4.2 Human activities and riverine carbon

Rivers annually deliver about 31.5 Tmol DIC, 19.1 Tmol DOC and 17.4 Tmol POC to the ocean (Table 3). Including 3.1 Tmol PIC/y increases the total riverine carbon export (TC) to 71.1 Tmol C/y, equating a contribution of 4 %, which is within the uncertainty of the estimates excluding PIC (Table 3). An accurate and precise knowledge of the riverine carbon export is necessary to understand the distribution and fate of anthropogenic carbon perturbations (Friedlingstein et al., 2020; Resplandy et al., 2018). Over the past century these riverine carbon fluxes have changed and continue doing so, likely in response to climate change and local human activities, such as industrialization, changes in land-use, hydrology and agricultural practices (Drake et al., 2018; Lambert et al., 2017; Li et al., 2019; Liu et al., 2020; Noacco et al., 2017; Raymond and Hamilton, 2018; van Hoek et al., 2021; Zeng et al., 2019).

The net effect of human activity on riverine sediment discharge is a ~10 % reduction, dominated by damming (Cohen et al., 2014; Syvitski et al., 2005), resulting in an even higher reduction of riverine PIC (~ 24 %, Table 3) and OC fluxes (~ 13 %, Maavara et al. (2017)). The differences between those fractions are related to the non-even spatial patterns of riverine carbon and sediment discharge (Ludwig et al., 1996; Milliman and Farnsworth, 2011, Figure 2). Damming also increases the residence time of particles in the riverine realm (Rueda et al., 2006), where PIC and POC are commonly remobilized by dissolution/degradation. However,

organic matter degradation and burial in reservoirs are very heterogeneous and dependent on reservoir ages (Maavara et al., 2017). Low importance for the model (- 2 %) for the extent water bodies, including reservoirs, indicate a rather negligible effect of reservoirs on PIC concentrations on the global scale. Our human factor is not an important predictor in the model (1 %), despite the expected influence of lime-fertilizers (Haynes and Naidu, 1998; Shoghi Kalkhoran et al., 2019; Zeng et al., 2019), of cement (Horvath, 2004), and of human-induced soil erosion, the latter affecting the active weathering zone (Govers et al., 2014). PIC could also be reduced by increasing dissolution through industrial or agricultural acids (Perrin et al., 2008; Webb and Sasowsky, 1994; Wicks and Groves, 1993). Eventually, the lack of resolution between those positive and negative influences in our human factor obscures a clearer relationship. Thus, more detailed studies on the different human influences on riverine carbonate are required. Notably, the human influence is correlated to observed PIC concentrations, but this spurious relationship stems from collinearity of SC and human population, both being high in southeast Asia, Europe and North America, confirming our method is correcting for multi-collinearity.

A 24 % reduction of PIC fluxes equates to only 1.4 % of the total riverine carbon flux (TC). The damming-related decrease in organic carbon fluxes (13 % of OC, Maavara et al. (2017)) results in another 6 % reduction of TC. In contrast, carbonate dissolution-related DIC fluxes likely increase(d) by ~ 13.5 % in the period 1950 – 2100 as a consequence of climate-change and land-use change (Zeng et al., 2019). Such an increase of DIC fluxes would result in a 5.6 % increase of TC, partially compensating the reduction of OC and PIC in terms of total carbon export (total disturbance: - 2 %). This is consistent with the estimation of a somewhat stable riverine TC export as a result of in-stream removal of anthropogenic carbon by POC deposition and respiration (Cole et al., 2007; Regnier et al., 2013; van Hoek et al., 2021).

The bulk anthropogenic effect on total global riverine DIC fluxes remains elusive

(Raymond and Hamilton, 2018) and human activities other than dam-building impact terrestrial and freshwater carbon cycling (van Hoek et al., 2021). Notably, humans also change conditions at the site of riverine PIC deposition: The current coastal ocean acidification in response to anthropogenic emissions and eutrophication (Borges and Gypens, 2010; Carstensen and Duarte, 2019) , could enhance PIC dissolution, acting as a heterogeneous buffer (Middelburg et al., 2020).

Table 3 *Summary of the riverine carbon export (in Tmol C/y). DIC: (Amiotte Suchet et al. (2003); Gaillardet et al. (1999); Hartmann et al. (2014); Li et al. (2017); Ludwig et al. (1996, 1998); Meybeck (1982), DOC: (Aitkenhead and McDowell (2000); Dai et al. (2012); Harrison et al. (2005); Li et al. (2019); Ludwig et al. (1996, 1998), POC: Beusen et al. (2005); Galy et al. (2015); Li et al. (2017); Ludwig et al. (1996, 1998); Meybeck (1982), Superscripts:* ^{S}*: By changes in sediment flux only,* ^{D}*: By damming only (Maavara et al., 2017; This study);* **: By climate change and land-use change for carbonate weathering only (Zeng et al., 2019). Human disturbance of TC is the bulk effect as indicated for DIC, PIC, DOC and POC. 'Literature' indicates averages and ranges taken from the above mentioned studies (grey columns). TC represents the sum of our PIC estimate and DIC, DOC and POC estimates from literature. Conversion to Pg/y by a factor 0.012011.*

	DIC	**PIC**	**DOC**	**POC**	**TC**
Modern global river export (Tmol C/y)	31.5	3.1	19.1	17.4	71.1
Percentage of TC	44.3	4.4	26.9	24.5	100
Range (Tmol C/y)	26.6 to 36.3	2.8 to 3.4	14.2 to 30.0	14.2 to 20.0	57.8 to 89.7
Human disturbance (%)	+13.5*	-24^{S}	-13^{D}	-13^{D}	- 2
Range (%)	+9.8 to +17.1	- 5.6 to - 39.0	-12.8 to -13.2	-12.8 to -13.2	-4 to + 0.7
Source	Literature	This study	Literature	Literature	This study & Literature

4.3 Implications for oceanic mass balances

The fate of the detrital carbonate flux in the marine realm, i.e., PIC burial or dissolution, determines the implication of the global PIC flux for oceanic mass balances (Middelburg et al., 2020). PIC preservation may affect global estimates of marine carbonate burial, while PIC

366 dissolution would translate to an additional input of Ca, Mg, Sr, C and alkalinity to the marine
367 solute inventories. Because the scientific community lacks a reliable global quantification of
368 these aspects, we discuss the following questions:

369 1. Where is river PIC deposited?

370 2. Does PIC deposition influence global estimates of carbonate burial?

371 3. Does PIC dissolve and alter oceanic mass balances of Ca, Mg, C, Sr and alkalinity?

372 **4.3.1 Where is river PIC deposited?**

373 On time scales of years to centuries, a major fraction of the riverine suspended matter remains
374 in the estuary (often ~ 40 - 60 %), while the rest is deposited along the shelves and continental
375 slopes with little escape towards the deep sea (Dyer, 1995; Meade, 1972; Wright and Nittrouer,
376 1995). However, sediment dynamics in river-dominated ocean margins are highly variable in
377 space and time, including deposition near the river mouth and subsequent lateral advection to
378 more calm environments as well as transport towards the slope (Geyer et al., 2004; McKee et
379 al., 2004). Saderne et al. (2019) emphasize that some coastal ecosystems, such as mangrove
380 forests and seagrass meadows, efficiently trap and dissolve such detrital carbonate from
381 external sources.

382 Global sea level fall under cooler climates (average Pleistocene state) exposes the PIC-
383 rich shelf to erosion, shifting depocenters to the slope, where PIC may be further transported
384 to and/or dissolved in the open ocean (Filippelli et al., 2007; Kump and Alley, 1994; Tsandev
385 et al., 2010). Thus, on larger time-scales (>10^3 years), most of the riverine PIC that does not
386 dissolve on short time-scale (1 to 10^2 years) will be transported to the slope. A significant
387 fraction may, however, have dissolved before re-mobilization or remain at the initial site of
388 deposition (preservation of the former estuary/shelf).

389 **4.3.2 Does PIC deposition influence global estimates of carbonate burial?**

Riverine PIC burial on the shelves may be implicitly included in carbonate mass accumulation (CMA) rate estimates derived from carbonate content, density and sediment accumulation rates, although microscopic criteria were established to distinguish biogenic and detrital carbonates (Milliman, 1974). However, hot spots of carbonate burial do generally not coincide very well with hot spots of riverine suspended sediment deposition (i.e., carbonate-poor shelves) (O'Mara and Dunne, 2019). Moreover, the dissolving PIC fraction and the fraction that remains at the initial site of deposition (i.e., is not re-eroded from the former estuary over longer time-scales) does not contribute to estimates of carbonate burial on the slope. Therefore, we believe that the effect of riverine PIC deposition on CMA-derived estimates of biogenic carbonate burial is rather limited. In contrast, carbonate burial estimates derived from mass balances (e.g., van der Ploeg et al., 2019) or solution chemistry (e.g., Chung et al., 2003) are directly affected by PIC dissolution.

4.3.3 Does PIC dissolve and alter oceanic mass balances of Ca, Mg, C, Sr and alkalinity?

Marine surface waters are supersaturated with respect to most carbonate minerals (Milliman, 1974; Peterson, 1966). Therefore, provision of carbonate mineral surfaces by PIC discharge, energetically favoring nucleation of these same minerals, may trigger inorganic carbonate precipitation in the water column (Wurgaft et al., 2016). TIC/TOC ratios of sediments from the Huanghe estuary, China (Gu et al., 2009; Yu et al., 2018), and trends in alkalinity/DIC ratios in the marginal Red Sea support this view (Wurgaft et al., 2016). Compared to marine carbonate compensation, PIC will rapidly settle in the shallow coastal ocean and the degree of carbonate saturation varies with depth and across different local environments at the seafloor (Aller, 1982; Boudreau and Canfield, 1993). As chemical conditions, especially pH, vary within the sediment column, carbonate may even be dissolved in the upper parts of the sediment column, but formed in the lower, more alkaline parts (Aller, 1994).

Carbonate dissolution at the sediment-water interface and in diagenetic settings is well

known (Aller, 1982; Archer et al., 1989; Sulpis et al., 2017). In these settings, aerobic degradation of organic matter may drive carbonate dissolution via the production of CO_2 and other acidic compounds (Aller, 1982; Oelkers et al., 2011). Anaerobic degradation produces reduced metabolites such as ammonium, sulfide and iron(II), most of which form strong acids upon upward migration and subsequent re-oxidation in the bioturbated zone, which drastically reduces carbonate saturation (Aller, 1994; Boudreau and Canfield, 1993) and may alter the carbon cycle-coupling of subsequent dissolution (Beaulieu et al., 2011; Huang et al., 2017; Liu et al., 2018; Torres et al., 2017).

Carbonate dissolution may also be influenced by biological activity such as seagrass root oxygen loss, sponge boring and bioturbation (Burdige et al., 2008; Mackenzie and Andersson, 2011; Saderne et al., 2019). Substantial riverine PIC dissolution was observed in the maximum turbidity zone of the eutrophic Loire estuary, France (Abril et al., 2003). Moreover, (detrital) carbonate dissolution driven by eutrophication-related bottom water acidification was observed in the Gulf of St. Lawrence, Canada (Nesbitt and Mucci, 2021) and in the Chesapeake Bay, USA (Shen et al., 2019). The proposed total flux of ~ 5 Tmol PIC/y corresponds to ~ 10 Tmol(eq)/a of alkalinity (~ 30 % of dissolved equivalent), which is ~ 30 % lower than the estimate of Middelburg et al. (2020). Despite integration of groundwater discharge, marine organic matter burial, anaerobic processes and marine silicate weathering, the modern ocean alkalinity budget is marked by an imbalance of ~25 % of the output by carbonate burial (59 Tmol(eq)/y in the coastal and open ocean). Half of this imbalance can be closed by inclusion of riverine PIC fluxes, assuming terrestrial PIC will either dissolve or biases estimates of carbonate burial (Graphical Abstract). Part of the residual imbalance could be attributed to other diagenetic processes in the coastal zone, such as marine alumo-silicates weathering (Gislason et al., 2006; Hong et al., 2020; Jones et al., 2012; Torres et al., 2020) and carbonate diagenesis (DePaolo, 2004; Fantle et al., 2010; Paytan et al., 2021). However, part of the

imbalance could be real, considering that the residence time of carbonate ions in the ocean (~ 100 ky) is larger then the time since the last glaciation (Middelburg et al., 2020; Milliman, 1993).

The inputs of ~5 Tmol PIC/y (rivers + cryosphere) further imply ~4.75 Tmol Ca/y, ~0.25 Tmol Mg/y and ~5 Gmol Sr/y, assuming ideal stoichiometry, 10 % dolomite (typical value in *GloRiSe* v1.1) and 1000 ppm Sr in calcite and dolomite. This equates to ~34.7 % (Ca), ~4.6 % (Mg) and ~8.9 % (Sr) of the respective dissolved equivalents, representing the current major input terms of the respective marine mass balances (Berner and Berner, 2012; Krabbenhöft et al., 2010; Mayfield et al., 2021; Tipper et al., 2010, 2006). As dolomites typically exhibit much lower dissolution rates than calcites (Pokrovsky et al., 2005), Mg addition by PIC dissolution is probably even smaller and thus negligible. So far, none of these highly discussed budgets could be consensually balanced, neither at the present state nor in reconstructions of the past – a conundrum persisting already for decades (Berner and Berner, 2012, 1987; Hong et al., 2020; Jones et al., 2012; Krabbenhöft et al., 2010; Mayfield et al., 2021; Middelburg et al., 2020; Milliman, 1993; Shalev et al., 2019; Tipper et al., 2006, 2010).

Riverine PIC input also impacts the Ca-cycle (Figure 5). Apart from riverine dissolved Ca fluxes, submarine groundwater discharge (1 Tmol Ca/yr, Mayfield et al., 2021) and hydrothermal processes (2 - 3 Tmol Ca/yr, DePaolo, 2004) were invoked to balance the high output fluxes by carbonate burial, but still leave an imbalane of 36 %, that can be reduced by further 16 % through consideration of PIC fluxes. The remaining 20 % could be attributed to submarine weathering of volcanogenic silicate debris (Gislason et al., 2006; Hong et al., 2020; Jones et al., 2012; Torres et al., 2020) and/or carbonate diagenesis (3 - 5 Tmol Ca/yr, DePaolo, 2004; Fantle et al., 2010). However, carbonate precipitation in early diagenetic settings currently represents an additional sink of ~ 1 Tmol Ca/yr and ~ 2 Tmol(eq)/y of alkalinity and is related to anaerobic oxidation of organic matter and silicate weathering (Schrag, 2013; Sun

and Turchyn, 2014; Torres et al., 2020). This flux is implicitly included into the mass balance of alkalinity (Graphical Abstract), by reducing the alkalinity source of the diagenetic reflux through carbonate dissolution (from DePaolo, 2004).

The fraction of detrital carbonates in coastal margin sediments was estimated to < 10 and 50 % in the Bengal fan (France-Lanord et al., 2018) and in the Gulf of Lyon (Pasquier et al., 2019), respectively. If the long-term biogenic carbonate burial on the slope is ~2 Tmol C/y (Milliman, 1993) and all riverine PIC (natural: 4.1 Tmol C/y) either dissolves or is transported

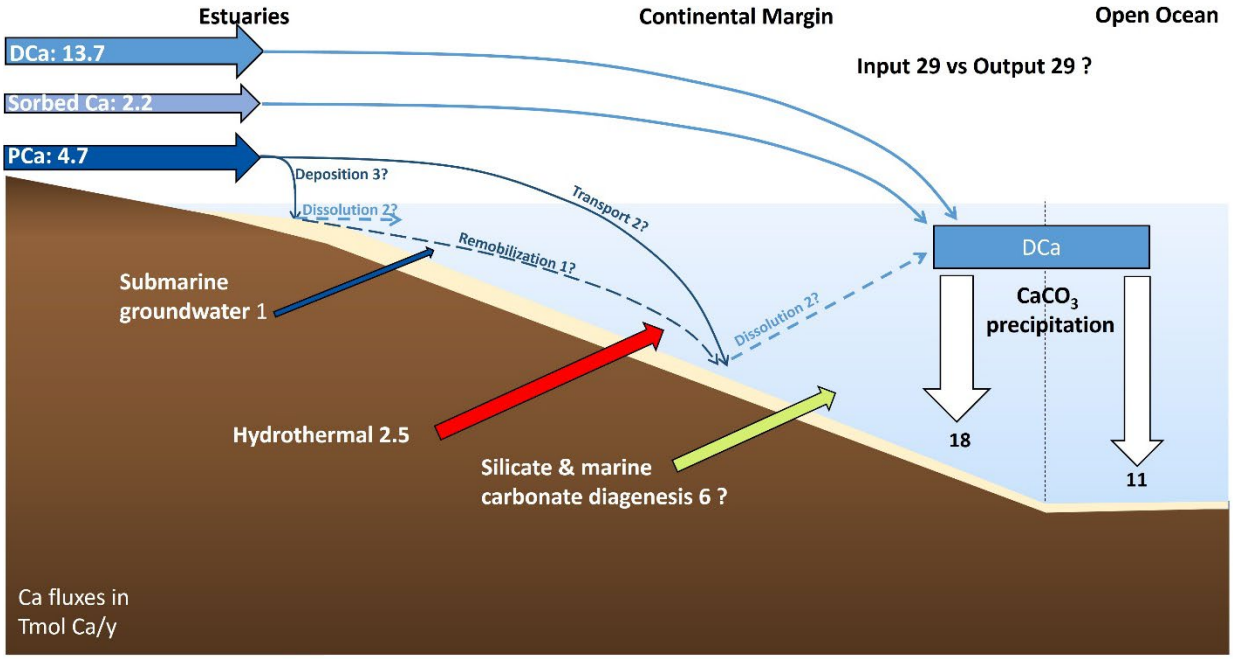

Figure 5 *Illustration of the modern ocean calcium budget and how it may be complemented by the inclusion of the riverine PCa flux. The fate of PCa (particulate Ca) in the ocean is, however, uncertain (details in the main text). Fluxes are given in Tmol Ca/y. $CaCO_3$ burial fluxes are from Middelburg et al. (2020), Milliman (1993) and O'Mara and Dunne (2019). River sorbed Ca is from Müller et al., (2021), DCa (dissolved Calcium) and groundwater inputs are from Mayfield et al. (2021), the hydrothermal flux and marine carbonate diagenesis (3 – 4 Tmol Ca/yr)is from DePaolo (2004). The silicate diagenesis flux of Ca is assumed to fill the residual imbalance of ~ 2 Tmol Ca/yr.*

to the slope on long time-scales, then 2.1 to 3.9 Tmol PIC/y (51 – 95 %) would need to dissolve in order to match these detrital fractions. This back-of-the-envelop calculation is not a valid quantification of the globally dissolving PIC fraction, but illustrates PIC dissolution may

indeed be significant. However, as argued above, the coastal ocean is a heterogeneous region with locally very spatio-temporally variable conditions supporting carbonate dissolution, preservation as well as precipitation. Importantly, recrystallization still leads to an exchange with the marine element and isotope inventories (e.g., Fantle et al., 2010; Kastner, 1999; Paytan et al., 2021). A global estimation of the dissolving PIC fraction should account of this spatio-temporal variability and complex interactions of organic and inorganic particles within coastal sediments. Therefore, consideration of the detrital mineral flux of rivers to the ocean and its isotopic composition may help to solve longwithstanding debates about imbalances in global biogeochemical cycles.

5 Next steps

Improving our understanding of the role of PIC in global biogeochemical cycles involves a qualitative understanding and quantitative estimation of its fate in the marine realm, as discussed in the previous section. This might be accomplished by tracing detrital components through isotopic approaches (e.g., France-Lanord et al., 2018; Pasquier et al., 2019) and by diagenetic modeling of riverine particles involving all the important biogeochemical processes driving carbonate precipitation an dissolution (Meister et al., 2022; Torres et al., 2020).

Apart from this, the accuracy of the modeled riverine PIC concentration needs to be improved. As seen from Figure 3, the ‘Source Carbonate’ is the most important predictor used in the model, but it is also the least well constrained, critically increasing the relative misfit at high concentrations and downward biasing at low concentrations (Figure 6) This might be improved by a more thorough assignment of carbonate content to the different lithological and unconsolidated sediment units through integration of chemical or mineralogical analysis into the corresponding maps. However, limited precision of low concentration measurements might pose an analytical limitation. In highly forested regions, PIC concentrations seem to be

systematically underestimated, which might be related to the type of forest. There is no obvious correlation of residuals to other important predictors (elevation, precipitation and bare areas), suggesting these variables are reasonably well captured. However, as discussed in section 4.2 (Human activities and riverine carbon), the human factor used in this study is rather vague (Table 1) and might mask certain opposing effects, such as liming or locally increased dissolution by acid introduction. Therefore, a detailed analysis of these factors would be warranted.

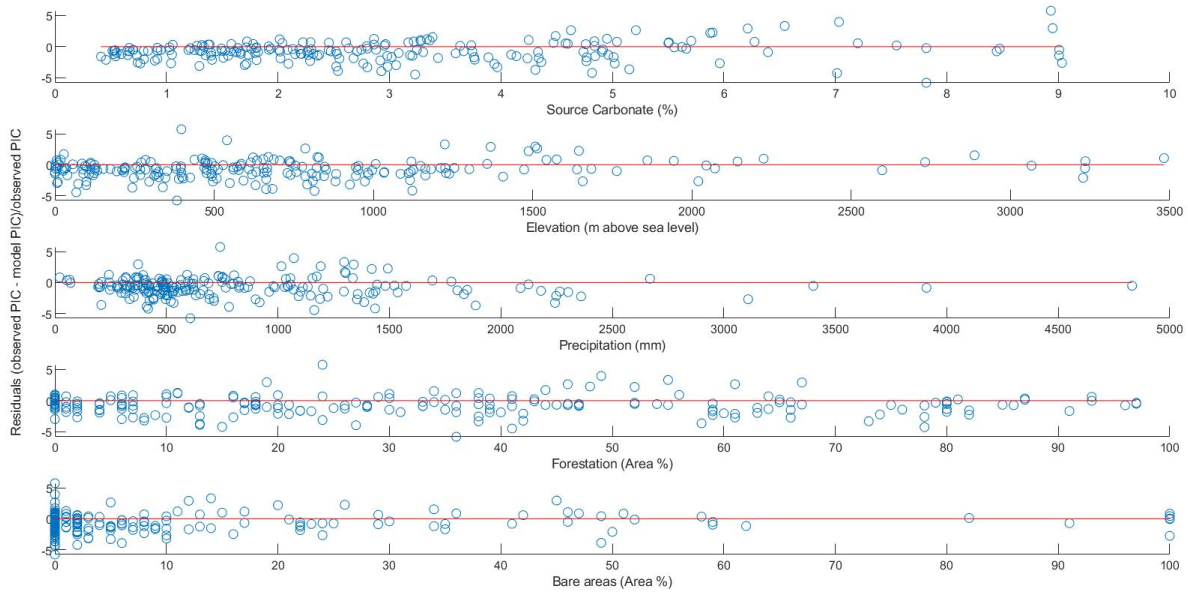

Figure 6 *Analysis of distribution of relative residuals (fractional deviation from observations) among the most important predictors in the model.*

Another important feature may be the accuracy and precision of measured PIC concentrations, as most studies on sediment composition do not involve PIC analysis, or at least do not report the carbonate content that was removed during sample preparation of organic carbon analysis (Müller et al., 2021a). A greater spatial and temporal (time series) coverage of such observations, especially in remote regions, such as Greenland and Antarctica, assist a more accurate upscaling. Similarly, vertically integrated sediment flux measurements, including estimates of bed load transport, could improve the quantification of not only PIC, but all river sediment related biogeochemical fluxes (e.g., Galy and France-Lanord, 2001). Finally,

contributions of Arctic continental ice-rafting and from coastal erosion to PIC fluxes could be significant and lack any reliable estimate.

6 Conclusion

The riverine flux of PIC, i.e., discharge of detrital carbonate minerals, represents a significant, yet mostly unaccounted chemical mass transfer in the Earth system (3.1 ± 0.3 Tmol C/y), currently contributing ~4.4 % to the total riverine carbon export. The pre-human flux was 4.1 ± 0.5 Tmol PIC/y; the 24 % reduction is caused by particle retention in reservoirs, especially of the Nile river. Considering perturbations of riverine particulate and dissolved, inorganic and organic carbon species in concert, the riverine export flux seems to have remained rather stable, while carbon speciation changed.

Although the fate of PIC in the ocean remains quantitatively unknown, oceanic element and isotope inventories of Ca and alkalinity are most probably affected by detrital carbonate dissolution in the coastal ocean, with implications for conclusions deduced from their highly debated, but frequently used mass balances. PIC contributions to the oceanic budgets of Sr and total C are less important and Mg fluxes are insignificant.

Naturally, the concentration of PIC is controlled by catchment topography and surface lithology, i.e., slowly changing tectonic factors (10^3 – 10^5 y scales), but also by climate and vegetation, which are subjected to much faster spatio-temporal variations. Similarly, marine conditions change through time, so that related PIC dissolution may also vary. An additional, significant amount of detrital carbonate (0.8 ± 0.3 Tmol C/y) is exported from Greenland and Antarctica and responds to ice-sheet dynamics, while eolian contributions can be neglected (at the present). These results imply a response of the global PIC flux to human activity and to natural changes in environmental and climatic conditions, but also to the tectonic evolution of our planet.

7 Data and script accessibility

All data and scripts used for this study, along with a detailed manual and the supplementary information, can can be accessed via: https://doi.org/10.5281/zenodo.6125880 (DOI: 10.5281/zenodo.6125880). Data from which figures were generated are can also be found as supplementary information alongside the online version of this article.

8 Competing Interest

The authors declare that they have no conflict in interest.

9 Funding

This work was carried out under the umbrella of the Netherlands Earth System Science Centre (NESSC). This project has received funding from the European Union's Horizon 2020 research and innovation programme under the Marie Skłodowska-Curie, grant agreement No 847504. Funding was also provided by BMBF-project PALMOD (Ref 01LP1506C) through the German Federal Ministry of Education and Research (BMBF) as Research for Sustainability inititative (FONA). AS thanks the European Research Council for Consolidator Grant 771497.

10 Acknowledgements

We thank Olivier Sulpis, Jens Hartmann, Gibran Romero-Mujalli, Stefan Kempe and Jaap Nienhuis for discussion and advice. Robert Hilton and and anonymous reviewer are thanked for their valuable inputs, significantly improving this work.

11 References

Abbott, A.N., Löhr, S., Trethewy, M., 2019. Are clay minerals the primary control on the oceanic rare earth element budget? Front. Mar. Sci. 6, 1–19. https://doi.org/10.3389/fmars.2019.00504

Abril, G., Etcheber, H., Delille, B., Frankignoulle, M., Borges, A. V., 2003. Carbonate dissolution in the turbid and eutrophic Loire estuary. Mar. Ecol. Prog. Ser. 259, 129–138.

https://doi.org/10.3354/meps259129

Aitkenhead, J.A., McDowell, W.H., 2000. Soil C:N ratio as a predictor of annual riverine DOC flux at local and global scales. Global Biogeochem. Cycles 14, 127–138. https://doi.org/10.1029/1999GB900083

Aller, R.C., 1994. Bioturbation and remineralization of sedimentary organic matter: effects of redox oscillation. Chem. Geol. 114, 331–345. https://doi.org/10.1016/0009-2541(94)90062-0

Aller, R.C., 1982. Carbonate dissolution in nearshore terrigenous muds: the role of physical and biological reworking. J. Geol. 90, 79–95. https://doi.org/10.1086/628652

Amiotte Suchet, P., Probst, J.-L., Ludwig, W., 2003. Worldwide distribution of continental rock lithology: Implications for the atmospheric/soil CO 2 uptake by continental weathering and alkalinity river transport to the oceans . Global Biogeochem. Cycles 17, n/a-n/a. https://doi.org/10.1029/2002gb001891

Archer, D., Emerson, S., Reimers, C., 1989. Dissolution of calcite in deep-sea sediments: pH and O2 microelectrode results. Geochim. Cosmochim. Acta 53, 2831–2845. https://doi.org/10.1016/0016-7037(89)90161-0

Batjes, N.H., 2012. ISRIC-WISE derived soil properties on a 5 by 5 arc-minutes global grid (ver. 1.2), ISRIC report. ISRIC - World Soil Information.

Bayon, G., Toucanne, S., Skonieczny, C., André, L., Bermell, S., Cheron, S., Dennielou, B., Etoubleau, J., Freslon, N., Gauchery, T., Germain, Y., Jorry, S.J., Ménot, G., Monin, L., Ponzevera, E., Rouget, M.L., Tachikawa, K., Barrat, J.A., 2015. Rare earth elements and neodymium isotopes in world river sediments revisited, Geochimica et Cosmochimica Acta. https://doi.org/10.1016/j.gca.2015.08.001

Beaulieu, E., Goddéris, Y., Labat, D., Roelandt, C., Calmels, D., Gaillardet, J., 2011. Modeling of water-rock interaction in the Mackenzie basin: Competition between sulfuric and carbonic acids. Chem. Geol. 289, 114–123. https://doi.org/10.1016/j.chemgeo.2011.07.020

Berner, E.K., Berner, R.A., 2012. Global environment : water, air, and geochemical cycles, 2nd ed. Princeton University Press, Princeton, N.J.

Berner, R.A., 1999. A New Look at the Long-term Carbon Cycle. Gsa Today 9, 1–6.

Berner, R.A., 1982. Burial of organic carbon and pyrite sulfur in the modern ocean. Am. J. Sci. 282, 451–473.

Berner, R.A., Berner, E.K., 1987. Global environment: water, air, and geochemical cycles, 1st ed. Prentice-Hall, New Jersey.

Berner, R.A., Lasaga, A.C., Garrels, R.M., 1983. The carbonate-silicate geochemical cycle ans its effect on atmospheric carbon dioxide over the past 100 million years. Am. J. Sci. 641–683.

Beusen, A.H.W., Dekkers, A.L.M., Bouwman, A.F., Ludwig, W., Harrison, J., 2005. Estimation of global river transport of sediments and associated particulate C, N, and P. Global Biogeochem. Cycles 19. https://doi.org/10.1029/2005GB002453

Bond, G.C., Lotti, R., 1995. Iceberg discharges into the North Atlantic on millennial time scales during the last glaciation. Science (80-.). 267, 1005–1010. https://doi.org/10.1126/science.267.5200.1005

Borges, A. V., Gypens, N., 2010. Carbonate chemistry in the coastal zone responds more strongly to eutrophication than to ocean acidification. Limnol. Oceanogr. 55, 346–353.

https://doi.org/10.4319/lo.2010.55.1.0346

Börker, J., Hartmann, J., Amann, T., Romero-Mujalli, G., 2018. Terrestrial sediments of the earth: Development of a global unconsolidated sediments map database (gum). Geochemistry, Geophys. Geosystems 19, 997–1024. https://doi.org/10.1002/2017GC007273

Bouchez, J., Gaillardet, J., France-Lanord, C., Maurice, L., Dutra-Maia, P., 2011. Grain size control of river suspended sediment geochemistry: Clues from Amazon River depth profiles. Geochemistry, Geophys. Geosystems 12, 1–24. https://doi.org/10.1029/2010GC003380

Boudreau, B.P., Canfield, D.E., 1993. A comparison of closed- and open-system models for porewater pH and calcite-saturation state. Geochim. Cosmochim. Acta 57, 317–334. https://doi.org/10.1016/0016-7037(93)90434-X

Boyer, E.W., Howarth, R.W., 2008. Nitrogen Fluxes from Rivers to the Coastal Oceans. Nitrogen Mar. Environ. 1565–1587. https://doi.org/10.1016/B978-0-12-372522-6.00036-0

Brantley, S.L., Eissenstat, D.M., Marshall, J.A., Godsey, S.E., Balogh-Brunstad, Z., Karwan, D.L., Papuga, S.A., Roering, J., Dawson, T.E., Evaristo, J., Chadwick, O., McDonnell, J.J., Weathers, K.C., 2017. Reviews and syntheses: On the roles trees play in building and plumbing the critical zone. Biogeosciences 14, 5115–5142. https://doi.org/10.5194/bg-14-5115-2017

Brantley, S.L., White, A.F., Kubicki, J.D., 2008. Kinetics of water-rock interaction, Kinetics of Water-Rock Interaction. https://doi.org/10.1007/978-0-387-73563-4

Broecker, W.S., 1982. Glacial to interglacial changes in ocean chemistry. Prog. Oceanogr. 11, 151–197. https://doi.org/10.1016/0079-6611(82)90007-6

Bufe, A., Hovius, N., Emberson, R., Rugenstein, J.K.C., Galy, A., Hassenruck-Gudipati, H.J., Chang, J.-M., 2021. Co-variation of silicate, carbonate, and sulphide weathering drives CO2-release with erosion. Nat. Geosci. 14, 211–216. https://doi.org/10.1038/s41561-021-00714-3

Burdige, D.J., Zimmerman, R.C., Hu, X., 2008. Rates of carbonate dissolution in permeable sediments estimated from pore-water profiles: The role of sea grasses. Limnol. Oceanogr. 53, 549–565. https://doi.org/10.4319/lo.2008.53.2.0549

Cai, W.J., Hu, X., Huang, W.J., Murrell, M.C., Lehrter, J.C., Lohrenz, S.E., Chou, W.C., Zhai, W., Hollibaugh, J.T., Wang, Y., Zhao, P., Guo, X., Gundersen, K., Dai, M., Gong, G.C., 2011. Acidification of subsurface coastal waters enhanced by eutrophication. Nat. Geosci. 4, 766–770. https://doi.org/10.1038/ngeo1297

Calmels, D., Gaillardet, J., Brenot, A., France-Lanord, C., 2007. Sustained sulfide oxidation by physical erosion processes in the Mackenzie River basin: Climatic perspectives. Geology 35, 1003–1006. https://doi.org/10.1130/G24132A.1

Calmels, D., Gaillardet, J., François, L., 2014. Sensitivity of carbonate weathering to soil CO2 production by biological activity along a temperate climate transect. Chem. Geol. 390, 74–86. https://doi.org/10.1016/j.chemgeo.2014.10.010

Canfield, D.E., 1997. The geochemistry of river particulates from the continental USA: Major elements. Geochim. Cosmochim. Acta 61, 3349–3365. https://doi.org/10.1016/S0016-7037(97)00172-5

Carstensen, J., Duarte, C.M., 2019. Drivers of pH Variability in Coastal Ecosystems. Environ. Sci. Technol. 53, 4020–4029. https://doi.org/10.1021/acs.est.8b03655

Caves Rugenstein, J.K., Ibarra, D.E., von Blanckenburg, F., 2019. Neogene cooling driven by land surface reactivity rather than increased weathering fluxes. Nature 571, 99–102.

https://doi.org/10.1038/s41586-019-1332-y

Chen, C., Guerit, L., Foreman, B.Z., Hassenruck-Gudipati, H.J., Adatte, T., Honegger, L., Perret, M., Sluijs, A., Castelltort, S., 2018. Estimating regional flood discharge during Palaeocene-Eocene global warming. Sci. Rep. 8, 1–8. https://doi.org/10.1038/s41598-018-31076-3

Chung, S.-N., Lee, K., Feely, R.A., Sabine, C.L., Millero, F.J., Wanninkhof, R., Bullister, J.L., Key, R.M., Peng, T.-H., 2003. Calcium carbonate budget in the Atlantic Ocean based on water column inorganic carbon chemistry. Global Biogeochem. Cycles 17, n/a-n/a. https://doi.org/10.1029/2002gb002001

Cohen, S., Kettner, A.J., Syvitski, J.P.M., 2014. Global suspended sediment and water discharge dynamics between 1960 and 2010: Continental trends and intra-basin sensitivity. Glob. Planet. Change 115, 44–58. https://doi.org/10.1016/j.gloplacha.2014.01.011

Cohen, S., Kettner, A.J., Syvitski, J.P.M., 2013. WBMsed , a distributed global-scale riverine sediment flux model : Model description and validation. Comput. Geosci. 53, 80–93. https://doi.org/10.1016/j.cageo.2011.08.011

Cole, J.J., Prairie, Y.T., Caraco, N.F., McDowell, W.H., Tranvik, L.J., Striegl, R.G., Duarte, C.M., Kortelainen, P., Downing, J.A., Middelburg, J.J., Melack, J., 2007. Plumbing the global carbon cycle: Integrating inland waters into the terrestrial carbon budget. Ecosystems 10, 171–184. https://doi.org/10.1007/s10021-006-9013-8

Conley, D.J., 2002. Terrestrial ecosystems and the global biogeochemical silica cycle. Global Biogeochem. Cycles 16, 68-1-68–8. https://doi.org/10.1029/2002gb001894

Dai, M., Yin, Z., Meng, F., Liu, Q., Cai, W.J., 2012. Spatial distribution of riverine DOC inputs to the ocean: An updated global synthesis. Curr. Opin. Environ. Sustain. 4, 170–178. https://doi.org/10.1016/j.cosust.2012.03.003

DePaolo, D.J., 2004. Calcium isotopic variations produced by biological, kinetic, radiogenic and nucleosynthetic processes. Rev. Mineral. Geochemistry 55, 255–288. https://doi.org/10.2138/gsrmg.55.1.255

Dickens, G.R., 2001. Carbon addition and removal during the late Palaeocene thermal maximum: Basic theory with a preliminary treatment of the isotopic record at ODP Site 1051, Blake Nose. Geol. Soc. Spec. Publ. 183, 293–305. https://doi.org/10.1144/GSL.SP.2001.183.01.14

Dixon, J.L., Chadwick, O.A., Vitousek, P.M., 2016. Climate-driven thresholds for chemical weathering in postglacial soils of New Zealand Jean. J. Geophys. Res. Earth Surf. Res. 1619–1634. https://doi.org/doi:10.1002/2016JF003864

Dixon, J.L., von Blanckenburg, F., 2012. Soils as pacemakers and limiters of global silicate weathering. Comptes Rendus - Geosci. 344, 597–609. https://doi.org/10.1016/j.crte.2012.10.012

Dornblaser, M.M., Striegl, R.G., 2009. Suspended sediment and carbonate transport in the Yukon River Basin, Alaska: Fluxes and potential future responses to climate change. Water Resour. Res. 45. https://doi.org/10.1029/2008WR007546

Drake, T.W., Tank, S.E., Zhulidov, A. V., Holmes, R.M., Gurtovaya, T., Spencer, R.G.M., 2018. Increasing Alkalinity Export from Large Russian Arctic Rivers. Environ. Sci. Technol. 52, 8302–8308. https://doi.org/10.1021/acs.est.8b01051

Dyer, K.R., 1995. Sediment transport processes in estuaries. Dev. Sedimentol. 53, 423–449. https://doi.org/10.1016/S0070-4571(05)80034-2

Ebelmen, J.-J., 1845. Sur les produits de la décomposition des espèces minérales de la famille des

691 silicates, in: Annales Des Mines. p. 66.

692 Fantle, M.S., Maher, K.M., Depaolo, D.J., 2010. Isotopic approaches for quantifying the rates of
693 marine burial diagenesis. Rev. Geophys. 48, 1–38. https://doi.org/10.1029/2009RG000306

694 Ferrier, K.L., West, N., 2017. Responses of chemical erosion rates to transient perturbations in
695 physical erosion rates, and implications for relationships between chemical and physical
696 erosion rates in regolith-mantled hillslopes. Earth Planet. Sci. Lett. 474, 447–456.
697 https://doi.org/10.1016/j.epsl.2017.07.002

698 Filippelli, G.M., Latimer, J.C., Murray, R.W., Flores, J.A., 2007. Productivity records from the Southern
699 Ocean and the equatorial Pacific Ocean: Testing the glacial Shelf-Nutrient Hypothesis. Deep.
700 Res. Part II Top. Stud. Oceanogr. 54, 2443–2452. https://doi.org/10.1016/j.dsr2.2007.07.021

701 Fletcher, D., MacKenzie, D., Villouta, E., 2005. Modelling skewed data with many zeros: A simple
702 approach combining ordinary and logistic regression. Environ. Ecol. Stat. 12, 45–54.
703 https://doi.org/10.1007/s10651-005-6817-1

704 Foreman, B.Z., Heller, P.L., Clementz, M.T., 2012. Fluvial response to abrupt global warming at the
705 Palaeocene/Eocene boundary. Nature 491, 92–95. https://doi.org/10.1038/nature11513

706 Foster, G.L., Vance, D., 2006. Negligible glacial-interglacial variation in continental chemical
707 weathering rates. Nature 444, 918–921. https://doi.org/10.1038/nature05365

708 France-Lanord, C., Galy, A., Rigaudier, T., 2018. Detrital, biogenic, and diagenetic carbonates in
709 turbidites of the Bengal Fan, in: Goldschmidt Conference 2018, Goldschmidt Abstracts. Boston,
710 United States.

711 Friedlingstein, P., O'Sullivan, M., Jones, M.W., Andrew, R.M., Hauck, J., Olsen, A., Peters, G.P., Peters,
712 W., Pongratz, J., Sitch, S., Le Quéré, C., Canadell, J.G., Ciais, P., Jackson, R.B., Alin, S., Aragão,
713 L.E.O.C., Arneth, A., Arora, V., Bates, N.R., Becker, M., Benoit-Cattin, A., Bittig, H.C., Bopp, L.,
714 Bultan, S., Chandra, N., Chevallier, F., Chini, L.P., Evans, W., Florentie, L., Forster, P.M., Gasser,
715 T., Gehlen, M., Gilfillan, D., Gkritzalis, T., Gregor, L., Gruber, N., Harris, I., Hartung, K., Haverd,
716 V., Houghton, R.A., Ilyina, T., Jain, A.K., Joetzjer, E., Kadono, K., Kato, E., Kitidis, V., Korsbakken,
717 J.I., Landschützer, P., Lefèvre, N., Lenton, A., Lienert, S., Liu, Z., Lombardozzi, D., Marland, G.,
718 Metzl, N., Munro, D.R., Nabel, J.E.M.S., Nakaoka, S.I., Niwa, Y., O'Brien, K., Ono, T., Palmer, P.I.,
719 Pierrot, D., Poulter, B., Resplandy, L., Robertson, E., Rödenbeck, C., Schwinger, J., Séférian, R.,
720 Skjelvan, I., Smith, A.J.P., Sutton, A.J., Tanhua, T., Tans, P.P., Tian, H., Tilbrook, B., Van Der Werf,
721 G., Vuichard, N., Walker, A.P., Wanninkhof, R., Watson, A.J., Willis, D., Wiltshire, A.J., Yuan, W.,
722 Yue, X., Zaehle, S., 2020. Global Carbon Budget 2020. Earth Syst. Sci. Data 12, 3269–3340.
723 https://doi.org/10.5194/essd-12-3269-2020

724 Froelich, P.N., Bender, M.L., Luedtke, N.A., Heath, G.R., DeVries, T., 1982. The marine phosphorous
725 cycle. Am. Journa Sci. 282, 474–511.

726 Gaillardet, J., Calmels, D., Romero-Mujalli, G., Zakharova, E., Hartmann, J., 2019. Global climate
727 control on carbonate weathering intensity. Chem. Geol. 527, 1–11.
728 https://doi.org/10.1016/j.chemgeo.2018.05.009

729 Gaillardet, J., Dupré, B., Allègre, C.J., 1999. Geochemistry of large river suspended sediments: Silicate
730 weathering or recycling tracer? Geochim. Cosmochim. Acta 63, 4037–4051.
731 https://doi.org/10.1016/s0016-7037(99)00307-5

732 Galy, A., France-Lanord, C., 2001. Higher erosion rates in the Himalaya: Geochemical constraints on
733 riverine fluxes. Geology 29, 23–26. https://doi.org/10.1130/0091-
734 7613(2001)029<0023:HERITH>2.0.CO;2

Galy, V., Peucker-Ehrenbrink, B., Eglinton, T., 2015. Global carbon export from the terrestrial biosphere controlled by erosion. Nature 521, 204–207. https://doi.org/10.1038/nature14400

Gandomi, A.H., Alavi, A.H., Ryan, C., 2015. Handbook of genetic programming applications, Handbook of Genetic Programming Applications. https://doi.org/10.1007/978-3-319-20883-1

Ganeshram, S., Pedersen, F., Calvert, E., Mcneill, W., Fontugne, M.R., 2000. in the world ' s oceans : Causes and consequences. Paleoceanography 15, 361–376.

Garzanti, E., Andó, S., France-Lanord, C., Censi, P., Vignola, P., Galy, V., Lupker, M., 2011. Mineralogical and chemical variability of fluvial sediments 2. Suspended-load silt (Ganga-Brahmaputra, Bangladesh). Earth Planet. Sci. Lett. 302, 107–120. https://doi.org/10.1016/j.epsl.2010.11.043

Gattuso, J.P., Frankignoulle, M., Wollast, R., 1998. Carbon and Carbonate Metabolism in Coastal Aquatic Ecosystems Author (s): J . -P . Gattuso , M . Frankignoulle and R . Wollast Source : Annual Review of Ecology and Systematics , Vol . 29 (1998), pp . 405-434 Published by : Annual Reviews Stable URL : Annu. Rev. Ecol. Syst. 29, 405–434.

Geyer, W.R., Hill, P.S., Kineke, G.C., 2004. The transport, transformation and dispersal of sediment by buoyant coastal flows. Cont. Shelf Res. 24, 927–949. https://doi.org/10.1016/j.csr.2004.02.006

Gislason, S.R., Oelkers, E.H., Snorrason, Á., 2006. Role of river-suspended material in the global carbon cycle. Geology 34, 49–52. https://doi.org/10.1130/G22045.1

Govers, G., Van Oost, K., Wang, Z., 2014. Scratching the Critical Zone: The Global Footprint of Agricultural Soil Erosion. Procedia Earth Planet. Sci. 10, 313–318. https://doi.org/10.1016/j.proeps.2014.08.023

Grosbois, C., Négrel, P., Grimaud, D., Fouillac, C., 2001. An overview of dissolved and suspended matter fluxes in the Loire River Basin: Natural and anthropogenic inputs. Aquat. Geochemistry 7, 81–105. https://doi.org/10.1023/A:1017518831860

Gu, D., Zhang, L., Jiang, L., 2009. The effects of estuarine processes on the fluxes of inorganic and organic carbon in the Yellow River estuary. J. Ocean Univ. China 8, 352–358. https://doi.org/10.1007/s11802-009-0352-x

Harrison, J.A., Caraco, N., Seitzinger, S.P., 2005. Global patterns and sources of dissolved organic matter export to the coastal zone: Results from a spatially explicit, global model. Global Biogeochem. Cycles 19. https://doi.org/10.1029/2005GB002480

Hartmann, J., Moosdorf, N., 2012. The new global lithological map database GLiM: A representation of rock properties at the Earth surface. Geochemistry, Geophys. Geosystems 13, 1–37. https://doi.org/10.1029/2012GC004370

Hartmann, J., Moosdorf, N., Lauerwald, R., Hinderer, M., West, A.J., 2014. Global chemical weathering and associated p-release - the role of lithology, temperature and soil properties. Chem. Geol. 363, 145–163. https://doi.org/10.1016/j.chemgeo.2013.10.025

Haynes, R.J., Naidu, R., 1998. Influence of lime, fertilizer and manure applications on soil organic matter. Nutr. Cycl. Agroecosystems 51, 123–137.

Hilton, R.G., West, A.J., 2020. Mountains, erosion and the carbon cycle. Nat. Rev. Earth Environ. 1, 284–299. https://doi.org/10.1038/s43017-020-0058-6

Hong, W.L., Torres, M.E., Kutterolf, S., 2020. Towards a global quantification of volcanogenic aluminosilicate alteration rates through the mass balance of strontium in marine sediments. Chem. Geol. 550, 119743. https://doi.org/10.1016/j.chemgeo.2020.119743

778 Horvath, A., 2004. Construction materials and the environment. Annu. Rev. Environ. Resour. 29,
779 181–204. https://doi.org/10.1146/annurev.energy.29.062403.102215

780 Huang, Q. bo, Qin, X. qun, Liu, P. yu, Zhang, L. kai, Su, C. tian, 2017. Impact of sulfuric and nitric acids
781 on carbonate dissolution, and the associated deficit of CO2 uptake in the upper–middle
782 reaches of the Wujiang River, China. J. Contam. Hydrol. 203, 18–27.
783 https://doi.org/10.1016/j.jconhyd.2017.05.006

784 Jeandel, C., Peucker-Ehrenbrink, B., Jones, M.T., Pearce, C.R., Oelkers, E.H., Godderis, Y., Lacan, F.,
785 Aumont, O., Arsouze, T., 2011. Ocean margins: The missing term in oceanic element budgets?
786 Eos (Washington. DC). 92, 217–218. https://doi.org/10.1029/2011EO260001

787 Jenny, H., 1941. Factors of soil formation: A System of Pedology, Soils: Basic Concepts and Future
788 Challenges. McGraw-Hill book Company, New York.
789 https://doi.org/10.1017/CBO9780511535802.014

790 Jickells, T.D., An, Z.S., Andersen, K.K., Baker, A.R., Bergametti, C., Brooks, N., Cao, J.J., Boyd, P.W.,
791 Duce, R.A., Hunter, K.A., Kawahata, H., Kubilay, N., LaRoche, J., Liss, P.S., Mahowald, N.,
792 Prospero, J.M., Ridgwell, A.J., Tegen, I., Torres, R., 2005. Global iron connections between
793 desert dust, ocean biogeochemistry, and climate. Science (80-.). 308, 67–71.
794 https://doi.org/10.1126/science.1105959

795 Jin, Y., Fu, W., Kang, J., Guo, Jiadong, Guo, Jian, 2019. Bayesian symbolic regression. arXiv.

796 Jones, M.T., Pearce, C.R., Jeandel, C., Gislason, S.R., Eiriksdottir, E.S., Mavromatis, V., Oelkers, E.H.,
797 2012. Riverine particulate material dissolution as a significant flux of strontium to the oceans.
798 Earth Planet. Sci. Lett. 355–356, 51–59. https://doi.org/10.1016/j.epsl.2012.08.040

799 Journet, E., Balkanski, Y., Harrison, S.P., 2014. A new data set of soil mineralogy for dust-cycle
800 modeling. Atmos. Chem. Phys. 14, 3801–3816. https://doi.org/10.5194/acp-14-3801-2014

801 Kastner, M., 1999. Oceanic minerals: Their origin, nature of their environment, and significance.
802 Proc. Natl. Acad. Sci. U. S. A. 96, 3380–3387. https://doi.org/10.1073/pnas.96.7.3380

803 Kempe, S., Emeis, K., 1985. Carboante Chemistry and the Formation of Plitvice Lake. Mitt. Geol.-
804 Paläont. Inst. Univ. Hambg. SCOPE/UNEP, 351–383.

805 Kitsikoudis, V., Sidiropoulos, E., Hrissanthou, V., 2013. Derivation of Sediment Transport Models for
806 Sand Bed Rivers from Data-Driven Techniques. Sediment Transp. Process. Their Model. Appl.
807 https://doi.org/10.5772/53432

808 Koehler, E., Brown, E., Haneuse, S.J.-P.A., 2009. On the Assessment of Monte Carlo Error in
809 Simulation-Based Statistical Analyses. Am. Stat. 63, 1-155–162.
810 https://doi.org/10.1198/tast.2009.0030.On

811 Krabbenhöft, A., Eisenhauer, A., Böhm, F., Vollstaedt, H., Fietzke, J., Liebetrau, V., Augustin, N.,
812 Peucker-Ehrenbrink, B., Müller, M.N., Horn, C., Hansen, B.T., Nolte, N., Wallmann, K., 2010.
813 Constraining the marine strontium budget with natural strontium isotope fractionations
814 (87Sr/86Sr*, δ88/86Sr) of carbonates, hydrothermal solutions and river waters. Geochim.
815 Cosmochim. Acta 74, 4097–4109. https://doi.org/10.1016/j.gca.2010.04.009

816 Krumins, V., Gehlen, M., Arndt, S., Van Cappellen, P., Regnier, P., 2013. Dissolved inorganic carbon
817 and alkalinity fluxes from coastal marine sediments: Model estimates for different shelf
818 environments and sensitivity to global change. Biogeosciences 10, 371–398.
819 https://doi.org/10.5194/bg-10-371-2013

820 Kump, L.R., Alley, R.B., 1994. Global chemical weathering on glacial time scales. Mater. Fluxes Surf.

Earth 46–60.

Kuylen, A.A.A., Verhallen, T.M.M., 1981. The use of canonical analysis. J. Econ. Psychol. 1, 217–237. https://doi.org/10.1016/0167-4870(81)90039-8

Lambert, T., Bouillon, S., Darchambeau, F., Morana, C., Roland, F.A.E., Descy, J.P., Borges, A. V., 2017. Effects of human land use on the terrestrial and aquatic sources of fluvial organic matter in a temperate river basin (The Meuse River, Belgium). Biogeochemistry 136, 191–211. https://doi.org/10.1007/s10533-017-0387-9

Lasaga, A.C., 1984. Chemical Kinetics of Water-Rock Interactions. J. Geophys. Res. 89, 4009–4025.

Lebrato, M., Garbe-Schönberg, D., Müller, M.N., Blanco-Ameijeiras, S., Feely, R.A., Lorenzoni, L., Molinero, J.C., Bremer, K., Jones, D.O.B., Iglesias-Rodriguez, D., Greeley, D., Lamare, M.D., Paulmier, A., Graco, M., Cartes, J., Barcelos e Ramos, J., de Lara, A., Sanchez-Leal, R., Jimenez, P., Paparazzo, F.E., Hartman, S.E., Westernströer, U., Küter, M., Benavides, R., da Silva, A.F., Bell, S., Payne, C., Olafsdottir, S., Robinson, K., Jantunen, L.M., Korablev, A., Webster, R.J., Jones, E.M., Gilg, O., du Bois, P.B., Beldowski, J., Ashjian, C., Yahia, N.D., Twining, B., Chen, X.G., Tseng, L.C., Hwang, J.S., Dahms, H.U., Oschlies, A., 2020. Global variability in seawater Mg:Ca and Sr:Ca ratios in the modern ocean. Proc. Natl. Acad. Sci. U. S. A. 117, 22281–22292. https://doi.org/10.1073/pnas.1918943117

Li, M., Peng, C., Wang, M., Xue, W., Zhang, K., Wang, K., Shi, G., Zhu, Q., 2017. The carbon flux of global rivers: A re-evaluation of amount and spatial patterns. Ecol. Indic. 80, 40–51. https://doi.org/10.1016/j.ecolind.2017.04.049

Li, M., Peng, C., Zhou, X., Yang, Y., Guo, Y., Shi, G., Zhu, Q., 2019. Modeling Global Riverine DOC Flux Dynamics From 1951 to 2015. J. Adv. Model. Earth Syst. 11, 514–530. https://doi.org/10.1029/2018MS001363

Linke, S., Lehner, B., Ouellet Dallaire, C., Ariwi, J., Grill, G., Anand, M., Beames, P., Burchard-Levine, V., Maxwell, S., Moidu, H., Tan, F., Thieme, M., 2019. Global hydro-environmental sub-basin and river reach characteristics at high spatial resolution. Sci. data 6, 283. https://doi.org/10.1038/s41597-019-0300-6

Liu, D., Bai, Y., He, X., Chen, C.T.A., Huang, T.H., Pan, D., Chen, X., Wang, D., Zhang, L., 2020. Changes in riverine organic carbon input to the ocean from mainland China over the past 60 years. Environ. Int. 134, 105258. https://doi.org/10.1016/j.envint.2019.105258

Liu, Z., Macpherson, G.L., Groves, C., Martin, J.B., Yuan, D., Zeng, S., 2018. Large and active CO2 uptake by coupled carbonate weathering. Earth-Science Rev. 182, 42–49. https://doi.org/10.1016/j.earscirev.2018.05.007

Ludwig, W., Amiotte-Suchet, P., Munhoven, G., Probst, J.L., 1998. Atmospheric CO2 consumption by continental erosion: Present-day controls and implications for the last glacial maximum. Glob. Planet. Change 16–17, 107–120. https://doi.org/10.1016/S0921-8181(98)00016-2

Ludwig, W., Amiotte-Suchet, P., Probst, J.L., 1996. River discharges of carbon to the world's oceans: Determining local inputs of alkalinity and of dissolved and particulate organic carbon. Comptes Rendus l'Academie Sci. - Ser. IIa Sci. la Terre des Planetes 323, 1007–1014.

Luo, M., Torres, M.E., Hong, W.L., Pape, T., Fronzek, J., Kutterolf, S., Mountjoy, J.J., Orpin, A., Henkel, S., Huhn, K., Chen, D., Kasten, S., 2020. Impact of iron release by volcanic ash alteration on carbon cycling in sediments of the northern Hikurangi margin. Earth Planet. Sci. Lett. 541, 116288. https://doi.org/10.1016/j.epsl.2020.116288

Ma, L., Jin, L., Brantley, S.L., 2011. Geochemical behaviors of different element groups during shale

865 weathering at the Susquehanna/Shale Hills Critical Zone Observatory. Appl. Geochemistry 26,
866 S89–S93. https://doi.org/10.1016/j.apgeochem.2011.03.038

867 Maavara, T., Lauerwald, R., Regnier, P., Van Cappellen, P., 2017. Global perturbation of organic
868 carbon cycling by river damming. Nat. Commun. 8, 1–10.
869 https://doi.org/10.1038/ncomms15347

870 Mackenzie, F.T., Andersson, A.J., 2011. Biological control on diagenesis: Influence of bacteria and
871 relevance to ocean acidification. Encycl. Earth Sci. Ser. 137–143. https://doi.org/10.1007/978-
872 1-4020-9212-1_73

873 Mackenzie, F.T., Garrels, R.M., 1966. Chemical mass balance between rivers and oceans. Am. J. Sci.
874 264, 507–525. https://doi.org/10.2475/ajs.264.7.507

875 Mackenzie, F.T., Garrels, R.M., 1965. Silicates : Reactivity with Sea Water Published by : American
876 Association for the Advancement of Science Stable URL :
877 https://www.jstor.org/stable/1717960 150, 57–58.

878 Mayfield, K.K., Eisenhauer, A., Santiago Ramos, D.P., Higgins, J.A., Horner, T.J., Auro, M., Magna, T.,
879 Moosdorf, N., Charette, M.A., Gonneea, M.E., Brady, C.E., Komar, N., Peucker-Ehrenbrink, B.,
880 Paytan, A., 2021. Groundwater discharge impacts marine isotope budgets of Li, Mg, Ca, Sr, and
881 Ba. Nat. Commun. 12, 1–9. https://doi.org/10.1038/s41467-020-20248-3

882 McKee, B.A., Aller, R.C., Allison, M.A., Bianchi, T.S., Kineke, G.C., 2004. Transport and transformation
883 of dissolved and particulate materials on continental margins influenced by major rivers:
884 Benthic boundary layer and seabed processes. Cont. Shelf Res. 24, 899–926.
885 https://doi.org/10.1016/j.csr.2004.02.009

886 Meade, R.H., 1972. Transport and Deposition of Sediments in Estuaries, in: Nelson, B.W. (Ed.),
887 Environmental Framework of Coastal Plain Estuaries.

888 Meister, P., Herda, G., Petrishcheva, E., Gier, S., Dickens, G.R., Bauer, C., Liu, B., 2022. Microbial
889 Alkalinity Production and Silicate Alteration in Methane Charged Marine Sediments:
890 Implications for Porewater Chemistry and Diagenetic Carbonate Formation. Front. Earth Sci. 9,
891 1–18. https://doi.org/10.3389/feart.2021.756591

892 Meybeck, M., 1993. C, N, P and S in Rivers: From Sources to Global Inputs BT - Interactions of C, N, P
893 and S Biogeochemical Cycles and Global Change I, 163–193.

894 Meybeck, M., 1982. Carbon, nitrogen, and phosphorus transport by world rivers. Am. J. Sci.
895 https://doi.org/10.2475/ajs.282.4.401

896 Middelburg, J.J., Soetaert, K., Hagens, M., 2020. Ocean Alkalinity, Buffering and Biogeochemical
897 Processes. Rev. Geophys. 58. https://doi.org/10.1029/2019RG000681

898 Milliman, J.D., 1993. Production and accumulation of calcium carbonate in the ocean: Budget of a
899 nonsteady state. Global Biogeochem. Cycles 7, 927–957.

900 Milliman, J.D., 1974. Marine carbonates, Springer. https://doi.org/10.1177/1464884910394285

901 Milliman, J.D., Farnsworth, K.L., 2011. River discharge to the coastal ocean: A global synthesis, River
902 Discharge to the Coastal Ocean: A Global Synthesis.
903 https://doi.org/10.1017/CBO9780511781247

904 Milliman, J.D., Syvitski, J.P.M., 1992. Geomorphic/tectonic control of sediment discharge to the
905 ocean: the importance of small mountainous rivers. J. Geol. 100, 525–544.
906 https://doi.org/10.1086/629606

907 Morse, J.W., Arvidson, R.S., 2002. The dissolution kinetics of major sedimentary carbonate minerals.
908 Earth-Science Rev. 58, 51–84. https://doi.org/10.1016/S0012-8252(01)00083-6

909 Mouyen, M., Longuevergne, L., Steer, P., Crave, A., Lemoine, J.M., Save, H., Robin, C., 2018.
910 Assessing modern river sediment discharge to the ocean using satellite gravimetry. Nat.
911 Commun. 9, 1–9. https://doi.org/10.1038/s41467-018-05921-y

912 Müller, G., Middelburg, J.J., Sluijs, A., 2021a. Global River Sediments (GloRiSe).
913 https://doi.org/10.5281/zenodo.4447435

914 Müller, G., Middelburg, J.J., Sluijs, A., 2021b. Introducing GloRiSe - A global database on river
915 sediment composition. Earth Syst. Sci. Data 13, 3565–3575.
916 https://doi.org/https://doi.org/10.5194/essd-13-3565-202

917 Négrel, P., Grosbois, C., 1999. Changes in chemical and 87Sr/86Sr signature distribution patterns of
918 suspended matter and bed sediments in the upper Loire river basin (France). Chem. Geol. 156,
919 231–249. https://doi.org/10.1016/S0009-2541(98)00182-X

920 Nesbitt, W.A., Mucci, A., 2021. Direct evidence of sediment carbonate dissolution in response to
921 bottom-water acidification in the gulf of st. Lawrence, canada. Can. J. Earth Sci. 58, 84–92.
922 https://doi.org/10.1139/cjes-2020-0020

923 Nienhuis, J.H., Ashton, A.D., Edmonds, D.A., Hoitink, A.J.F., Kettner, A.J., Rowland, J.C., Törnqvist,
924 T.E., 2020. Global-scale human impact on delta morphology has led to net land area gain.
925 Nature 577, 514–518. https://doi.org/10.1038/s41586-019-1905-9

926 Noacco, V., Wagener, T., Worrall, F., Burt, T.P., Howden, N.J.K., 2017. Human impact on long-term
927 organic carbon export to rivers. J. Geophys. Res. Biogeosciences 122, 947–965.
928 https://doi.org/10.1002/2016JG003614

929 O'Mara, N.A., Dunne, J.P., 2019. Hot Spots of Carbon and Alkalinity Cycling in the Coastal Oceans.
930 Sci. Rep. 9, 1–8. https://doi.org/10.1038/s41598-019-41064-w

931 Oelkers, E.H., Golubev, S. V., Pokrovsky, O.S., Bénézeth, P., 2011. Do organic ligands affect calcite
932 dissolution rates? Geochim. Cosmochim. Acta 75, 1799–1813.
933 https://doi.org/10.1016/j.gca.2011.01.002

934 Overeem, I., Hudson, B.D., Syvitski, J.P.M., Mikkelsen, A.B., Hasholt, B., Van Den Broeke, M.R., Noel,
935 B.P.Y., Morlighem, M., 2017. Substantial export of suspended sediment to the global oceans
936 from glacial erosion in Greenland. Nat. Geosci. 10, 859–863.
937 https://doi.org/10.1038/NGEO3046

938 Pasquier, V., Revillon, S., Leroux, E., Molliex, S., Mocochain, L., Rabineau, M., 2019. Quantifying
939 biogenic versus detrital carbonates on marine shelf: An isotopic approach. Front. Earth Sci. 7,
940 1–10. https://doi.org/10.3389/feart.2019.00164

941 Paytan, A., Griffith, E.M., Eisenhauer, A., Hain, M.P., Wallmann, K., Ridgwell, A., 2021. A 35-million-
942 year record of seawater stable Sr isotopes reveals a fluctuating global carbon cycle. Science
943 (80-.). 371, 1346–1350. https://doi.org/10.1126/science.aaz9266

944 Penman, D.E., Caves Rugenstein, J.K., Ibarra, D.E., Winnick, M.J., 2020. Silicate weathering as a
945 feedback and forcing in Earth's climate and carbon cycle. Earth-Science Rev. 209, 103298.
946 https://doi.org/10.1016/j.earscirev.2020.103298

947 Perrin, A.S., Probst, A., Probst, J.L., 2008. Impact of nitrogenous fertilizers on carbonate dissolution
948 in small agricultural catchments: Implications for weathering CO2 uptake at regional and global
949 scales. Geochim. Cosmochim. Acta 72, 3105–3123. https://doi.org/10.1016/j.gca.2008.04.011

Peterson, M.N.A., 1966. Calcite: Rates of dissolution in a vertical profile in the central pacific. Science (80-.). 154, 1542–1544. https://doi.org/10.1126/science.154.3756.1542

Pokrovsky, O.S., Golubev, S. V., Schott, J., 2005. Dissolution kinetics of calcite, dolomite and magnesite at 25 °C and 0 to 50 atm pCO2. Chem. Geol. 217, 239–255. https://doi.org/10.1016/j.chemgeo.2004.12.012

Poulton, S.W., Raiswell, R., 2002. The low-temperature geochemical cycle of iron: From continental fluxes to marine sediment deposition. Am. J. Sci. 302, 774–805. https://doi.org/10.2475/ajs.302.9.774

Raiswell, R., Benning, L.G., Tranter, M., Tulaczyk, S., 2008. Bioavailable iron in the Southern Ocean: The significance of the iceberg conveyor belt. Geochem. Trans. 9, 1–9. https://doi.org/10.1186/1467-4866-9-7

Raymond, P.A., Hamilton, S.K., 2018. Anthropogenic influences on riverine fluxes of dissolved inorganic carbon to the oceans. Limnol. Oceanogr. Lett. 3, 143–155. https://doi.org/10.1002/lol2.10069

Regnier, P., Friedlingstein, P., Ciais, P., Mackenzie, F.T., Gruber, N., Janssens, I.A., Laruelle, G.G., Lauerwald, R., Luyssaert, S., Andersson, A.J., Arndt, S., Arnosti, C., Borges, A. V., Dale, A.W., Gallego-Sala, A., Goddéris, Y., Goossens, N., Hartmann, J., Heinze, C., Ilyina, T., Joos, F., Larowe, D.E., Leifeld, J., Meysman, F.J.R., Munhoven, G., Raymond, P.A., Spahni, R., Suntharalingam, P., Thullner, M., 2013. Anthropogenic perturbation of the carbon fluxes from land to ocean. Nat. Geosci. 6, 597–607. https://doi.org/10.1038/ngeo1830

Resplandy, L., Keeling, R.F., Rödenbeck, C., Stephens, B.B., Khatiwala, S., Rodgers, K.B., Long, M.C., Bopp, L., Tans, P.P., 2018. Revision of global carbon fluxes based on a reassessment of oceanic and riverine carbon transport. Nat. Geosci. 11, 504–509. https://doi.org/10.1038/s41561-018-0151-3

Rovan, L., Zuliani, T., Horvat, B., Kanduč, T., Vreča, P., Jamil, Q., Čermelj, B., Bura-Nakić, E., Cukrov, N., Štrok, M., Lojen, S., 2021. Uranium isotopes as a possible tracer of terrestrial authigenic carbonate. Sci. Total Environ. 797. https://doi.org/10.1016/j.scitotenv.2021.149103

Rueda, F., Moreno-Ostos, E., Armengol, J., 2006. The residence time of river water in reservoirs. Ecol. Modell. 191, 260–274. https://doi.org/10.1016/j.ecolmodel.2005.04.030

Saderne, V., Geraldi, N.R., Macreadie, P.I., Maher, D.T., Middelburg, J.J., Serrano, O., Almahasheer, H., Arias-Ortiz, A., Cusack, M., Eyre, B.D., Fourqurean, J.W., Kennedy, H., Krause-Jensen, D., Kuwae, T., Lavery, P.S., Lovelock, C.E., Marba, N., Masqué, P., Mateo, M.A., Mazarrasa, I., McGlathery, K.J., Oreska, M.P.J., Sanders, C.J., Santos, I.R., Smoak, J.M., Tanaya, T., Watanabe, K., Duarte, C.M., 2019. Role of carbonate burial in Blue Carbon budgets. Nat. Commun. 10. https://doi.org/10.1038/s41467-019-08842-6

Santos, I.R., Maher, D.T., Larkin, R., Webb, J.R., Sanders, C.J., 2019. Carbon outwelling and outgassing vs. burial in an estuarine tidal creek surrounded by mangrove and saltmarsh wetlands. Limnol. Oceanogr. 64, 996–1013. https://doi.org/10.1002/lno.11090

Savenko, V.S., 2007. Chemical composition of sediment load carried by rivers. Geochemistry Int. 45, 816–824. https://doi.org/10.1134/S0016702907080071

Schachtman, N.S., Roering, J.J., Marshall, J.A., Gavin, D.G., Granger, D.E., 2019. The interplay between physical and chemical erosion over glacial-interglacial cycles. Geology 47, 613–616. https://doi.org/10.1130/G45940.1

Schrag, D.P., 2013. Authigenic carbonate and the history of the global carbon cycle. Science (80-.).

339, 540–543. https://doi.org/10.1126/science.339.6126.1383-b

Searson, D.P., Leahy, D.E., Willis, M.J., 2010. GPTIPS:An open source genetic programming toolbox for multigene symbolic regression. Proc. Int. MultiConference Eng. Comput. Sci. 2010, IMECS 2010 I, 77–80.

Shalev, N., Bontognali, T.R.R., Wheat, C.G., Vance, D., 2019. New isotope constraints on the Mg oceanic budget point to cryptic modern dolomite formation. Nat. Commun. 10, 1–10. https://doi.org/10.1038/s41467-019-13514-6

Shen, C., Testa, J.M., Li, M., Cai, W.J., Waldbusser, G.G., Ni, W., Kemp, W.M., Cornwell, J., Chen, B., Brodeur, J., Su, J., 2019. Controls on Carbonate System Dynamics in a Coastal Plain Estuary: A Modeling Study. J. Geophys. Res. Biogeosciences 124, 61–78. https://doi.org/10.1029/2018JG004802

Shoghi Kalkhoran, S., Pannell, D.J., Thamo, T., White, B., Polyakov, M., 2019. Soil acidity, lime application, nitrogen fertility, and greenhouse gas emissions: Optimizing their joint economic management. Agric. Syst. 176, 102684. https://doi.org/10.1016/j.agsy.2019.102684

Sluijs, A., Zeebe, R.E., Bijl, P.K., Bohaty, S.M., 2013. A middle Eocene carbon cycle conundrum. Nat. Geosci. 6, 429–434. https://doi.org/10.1038/ngeo1807

Sulpis, O., Lix, C., Mucci, A., Boudreau, B.P., 2017. Calcite dissolution kinetics at the sediment-water interface in natural seawater. Mar. Chem. 195, 70–83. https://doi.org/10.1016/j.marchem.2017.06.005

Sun, X., Turchyn, A. V., 2014. Significant contribution of authigenic carbonate to marine carbon burial. Nat. Geosci. 7, 201–204. https://doi.org/10.1038/ngeo2070

Sutton, J.N., André, L., Cardinal, D., Conley, D.J., Souza, G.F. De, Dean, J., Dodd, J., Ehlert, C., Ellwood, M.J., 2018. A Review of the Stable Isotope Bio-geochemistry of the Global Silicon Cycle and Its Associated Trace Elements 5. https://doi.org/10.3389/feart.2017.00112

Syvitski, J.P.M., Kettner, A., 2011. Sediment flux and the anthropocene. Philos. Trans. R. Soc. A Math. Phys. Eng. Sci. 369, 957–975. https://doi.org/10.1098/rsta.2010.0329

Syvitski, J.P.M., Vörösmarty, C.J., Kettner, A.J., Green, P., 2005. Impact of Humans on the Flux of Terrestrial Sediment to the Global Coastal Ocean. Science (80-.). 308, 376–381. https://doi.org/10.1126/science.1109454

Tipper, E.T., Gaillardet, J., Galy, A., Louvat, P., Bickle, M.J., Capmas, F., 2010. Calcium isotope ratios in the world's largest rivers: A constraint on the maximum imbalance of oceanic calcium fluxes. Global Biogeochem. Cycles 24. https://doi.org/10.1029/2009GB003574

Tipper, E.T., Galy, A., Gaillardet, J., Bickle, M.J., Elderfield, H., Carder, E.A., 2006. The magnesium isotope budget of the modern ocean: Constraints from riverine magnesium isotope ratios. Earth Planet. Sci. Lett. 250, 241–253. https://doi.org/10.1016/j.epsl.2006.07.037

Tipper, E.T., Stevenson, E.I., Alcock, V., Knight, A.C.G., Baronas, J.J., Hilton, R.G., Bickle, M.J., Larkin, C.S., Feng, L., Relph, K.E., Hughes, G., 2021. Global silicate weathering flux overestimated because of sediment-water cation exchange. Proc. Natl. Acad. Sci. U. S. A. 118. https://doi.org/10.1073/pnas.2016430118

Torres, M.A., Moosdorf, N., Hartmann, J., Adkins, J.F., West, A.J., 2017. Glacial weathering, sulfide oxidation, and global carbon cycle feedbacks. Proc. Natl. Acad. Sci. U. S. A. 114, 8716–8721. https://doi.org/10.1073/pnas.1702953114

Torres, M.A., West, A.J., Li, G., 2014. Sulphide oxidation and carbonate dissolution as a source of CO2

over geological timescales. Nature 507, 346–349. https://doi.org/10.1038/nature13030

Torres, M.E., Hong, W.L., Solomon, E.A., Milliken, K., Kim, J.H., Sample, J.C., Teichert, B.M.A., Wallmann, K., 2020. Silicate weathering in anoxic marine sediment as a requirement for authigenic carbonate burial. Earth-Science Rev. 200, 102960. https://doi.org/10.1016/j.earscirev.2019.102960

Tsandev, I., Rabouille, C., Slomp, C.P., Van Cappellen, P., 2010. Shelf erosion and submarine river canyons: Implications for deep-sea oxygenation and ocean productivity during glaciation. Biogeosciences 7, 1973–1982. https://doi.org/10.5194/bg-7-1973-2010

Urey, H., 1952. On the early chemical history of the earth and the origin of life. Geophysics 38, 351–363.

van de Schootbrugge, B., van der Weijst, C.M.H., Hollaar, T.P., Vecoli, M., Strother, P.K., Kuhlmann, N., Thein, J., Visscher, H., van Konijnenburg-van Cittert, H., Schobben, M.A.N., Sluijs, A., Lindström, S., 2020. Catastrophic soil loss associated with end-Triassic deforestation. Earth-Science Rev. 210, 103332. https://doi.org/10.1016/j.earscirev.2020.103332

van der Ploeg, R., Boudreau, B.P., Middelburg, J.J., Sluijs, A., 2019. Cenozoic carbonate burial along continental margins. Geology 47, 1025–1028. https://doi.org/10.1130/G46418.1

van Hoek, W.J., Wang, J., Vilmin, L., Beusen, A.H.W., Mogollón, J.M., Müller, G., Pika, P.A., Liu, X., Langeveld, J.J., Bouwman, A.F., Middelburg, J.J., 2021. Exploring Spatially Explicit Changes in Carbon Budgets of Global River Basins during the 20th Century. Environ. Sci. Technol. 55, 16757–16769. https://doi.org/10.1021/acs.est.1c04605

Viers, J., Dupré, B., Gaillardet, J., 2009. Chemical composition of suspended sediments in World Rivers: New insights from a new database. Sci. Total Environ. 407, 853–868. https://doi.org/10.1016/j.scitotenv.2008.09.053

Wadham, J.L., De'Ath, R., Monteiro, F.M., Tranter, M., Ridgwell, A., Raiswell, R., Tulaczyk, S., 2013. The potential role of the Antarctic Ice Sheet in global biogeochemical cycles. Earth Environ. Sci. Trans. R. Soc. Edinburgh 104, 55–67. https://doi.org/10.1017/S1755691013000108

Wallace, R.B., Baumann, H., Grear, J.S., Aller, R.C., Gobler, C.J., 2014. Coastal ocean acidification: The other eutrophication problem. Estuar. Coast. Shelf Sci. 148, 1–13. https://doi.org/10.1016/j.ecss.2014.05.027

Walz, J., Knoblauch, C., Böhme, L., Pfeiffer, E.M., 2017. Regulation of soil organic matter decomposition in permafrost-affected Siberian tundra soils - Impact of oxygen availability, freezing and thawing, temperature, and labile organic matter. Soil Biol. Biochem. 110, 34–43. https://doi.org/10.1016/j.soilbio.2017.03.001

Webb, J.A., Sasowsky, I.D., 1994. The interaction of acid mine drainage with a carbonate terrane: evidence from the Obey River, north-central Tennessee. J. Hydrol. 161.

West, A.J., Galy, A., Bickle, M., 2005. Tectonic and climatic controls on silicate weathering. Earth Planet. Sci. Lett. 235, 211–228. https://doi.org/10.1016/j.epsl.2005.03.020

West, J.A., 2012. Thickness of the chemical weathering zone and implications for erosional and climatic drivers of weathering and for carbon-cycle feedbacks. Geology 40, 811–814. https://doi.org/10.1130/G33041.1

White, L.F., Bailey, I., Foster, G.L., Allen, G., Kelley, S.P., Andrews, J.T., Hogan, K., Dowdeswell, J.A., Storey, C.D., 2016. Tracking the provenance of Greenland-sourced, Holocene aged, individual sand-sized ice-rafted debris using the Pb-isotope compositions of feldspars and 40Ar/39Ar ages

of hornblendes. Earth Planet. Sci. Lett. 433, 192–203. https://doi.org/10.1016/j.epsl.2015.10.054

Wicks, C.M., Groves, C.G., 1993. Acidic mine drainage in carbonate terrains: geochemical processes and rates of calcite dissolution. J. Hydrol. 146, 13–27. https://doi.org/10.1016/0022-1694(93)90267-D

Willenbring, J.K., Von Blanckenburg, F., 2010. Long-term stability of global erosion rates and weathering during late-Cenozoic cooling. Nature 465, 211–214. https://doi.org/10.1038/nature09044

Wright, L.D., Nittrouer, C.A., 1995. Dispersal of river sediments in coastal seas: Six contrasting cases. Estuaries 18, 494–508. https://doi.org/10.2307/1352367

Wurgaft, E., Steiner, Z., Luz, B., Lazar, B., 2016. Evidence for inorganic precipitation of CaCO3 on suspended solids in the open water of the Red Sea, Marine Chemistry. Elsevier B.V. https://doi.org/10.1016/j.marchem.2016.09.006

Yu, Z., Wang, X., Han, G., Liu, X., Zhang, E., 2018. Organic and inorganic carbon and their stable isotopes in surface sediments of the Yellow River Estuary. Sci. Rep. 8. https://doi.org/10.1038/s41598-018-29200-4

Zeng, S., Liu, Z., Kaufmann, G., 2019. Sensitivity of the global carbonate weathering carbon-sink flux to climate and land-use changes. Nat. Commun. 10, 1–10. https://doi.org/10.1038/s41467-019-13772-4

Zhao, M.Y., Zheng, Y.F., Zhao, Y.Y., 2016. Seeking a geochemical identifier for authigenic carbonate. Nat. Commun. 7, 1–7. https://doi.org/10.1038/ncomms10885

Zhou, Y.Q., Sawyer, A.H., David, C.H., Famiglietti, J.S., 2019. Fresh Submarine Groundwater Discharge to the Near-Global Coast. Geophys. Res. Lett. 46, 5855–5863. https://doi.org/10.1029/2019GL082749

Zolkos, S., Tank, S.E., Kokelj, S. V., 2018. Mineral Weathering and the Permafrost Carbon-Climate Feedback. Geophys. Res. Lett. 45, 9623–9632. https://doi.org/10.1029/2018GL078748

Zolkos, S., Tank, S.E., Striegl, R.G., Kokelj, S. V., Kokoszka, J., Estop-Aragonés, C., Olefeldt, D., 2020. Thermokarst amplifies fluvial inorganic carbon cycling and export across watershed scales on the Peel Plateau, Canada. Biogeosciences 17, 5163–5182. https://doi.org/10.5194/bg-17-5163-2020